Royal Netherlands
Meteorological Institute
Ministry of Infrastructure
and Water Management

KNMI Climate Scenarios for Suriname

E.C. Koole, N. Bloemendaal, M. Brotons, R. Haarsma, I. Keizer, D. Le Bars and H. de Vries

De Bilt, 2024| Scientific report; WR 24-01

KNMI Climate Scenarios for Suriname

E.C. Koole[1], N. Bloemendaal[1,2], M. Brotons[1,3], R. Haarsma[1,4], I. Keizer[1], D. Le Bars[1], and H. de Vries[1]

[1] *KNMI Royal Netherlands Meteorological Institute, de Bilt, the Netherlands*
[2] *Free University of Amsterdam (VU), Amsterdam, The Netherlands*
[3] *Universitat de Barcelona, Barcelona, Spain*
[4] *Barcelona Supercomputing Center (BSC), Barcelona, Spain*

Tuesday 15th October, 2024

Abstract

This report discusses the climate scenarios for Suriname that were developed within the Makandra - Early Warning program. Within these scenarios four variables are considered: temperature, precipitation, wind, and sea level rise (SLR). For all variables a framework is used that is similar to the KNMI National Climate Scenarios 2023 for the Netherlands (KNMI'23 scenario's) van Dorland et al. (2024), Chapter 9 on the Dutch Caribbean. As in the KNMI'23 scenario's a distinction between low (SSP1-2.6), medium (SSP2-4.5) and high (SSP5-8.5) emission pathways is made. For the variables temperature, precipitation and wind a further subdivision into a wet and dry trend scenario is made. The main findings of the climate scenarios for Suriname are:

Temperature: Warming continues in the high emission scenarios (Hd, Hn), reaching values up to +4K (coastal) and +5.5K (interior) (above current climatology) in 2100. In the low emission scenarios (Ld, Ln) the warming plateaus at +0.9K (coastal) and +1.1K (interior) around 2050, remaining approximately constant thereafter.

Precipitation: Large uncertainties, but overall a reduction is expected in total amount of precipitation annually. Reductions of around 30% (coastal) and 24% (interior) in 2100 in Hd; much smaller reductions in the wet scenario (Hn) and in all low emission scenarios. The dry (ASON) season is most likely to become drier and the wet (AMJJ) season can as a result of model uncertainty in the future both be drier or wetter on average than now.

Wind: Small increases of a few percent (max. increase in annual wind speed over the interior under Hd in 2100 is around 6%).

Sea level rise: Present-day rates of SLR are on the order of 4 mm/yr, which is faster than the global sea level rate of 3.4 mm/yr. These rates increase in all scenarios, resulting in an expected (median) increase of sea level at the coast of Suriname of +45 cm under SSP1-2.6 and +78 cm in SSP5-8.5 in 2100.

Note of caution: There is a discrepancy between observed and modelled historical trends. CMIP6 historic modelled trends show a systematic change towards more El Niño like conditions, whilst observed historical trends are tending towards La Niña like conditions. Natural variability cannot be ruled out completely, but there is a possibility that the models exhibit a systematic bias. CMIP6 models also project the ITCZ zone too far towards the south compared to observations.

Contents

1 Introduction

This report documents the climate scenarios for Suriname that were constructed within the collaboration project 'Early warning Suriname' between the meteorological service Suriname (MDS) and the Royal Netherlands Meteorological Institute (KNMI). The methodology and choices that are followed closely resemble that of the KNMI National Climate Scenarios 2023 (KNMI'23) for the Netherlands (van Dorland et al., 2024). This report analyses the past, present and future climate of Suriname. For the analysis of the past and present climate, our analysis relies on observational and reanalysis data. For the projected climate scenarios we use output from 29 Global Climate Models (GCMs) that are based on the Coupled Model Intercomparison Project (CMIP6) model runs. The complete reasoning behind the climate scenarios can be read in van Dorland et al. (2024), only a brief overview is given here.

The KNMI scenarios are designed to give a range of climate states/conditions to which Suriname might be exposed within the uncertainties of the future climate system and greenhouse gas emissions. A climate change scenario is the difference between a climate scenario and the current climate. This current climate is based upon the reference period 1991-2020; the most recent WMO climatological normal period. The time horizons for the climate scenarios are 2050 and 2100. These horizons are presented as a single year, but actually consist of the 30-year climatological values around this horizon year (for 2050 this is the period 2036-2065).

The climate system naturally varies in time. Within this variation, internal variability and forced variability are characterized, where the first are natural variations of the climate system on many timescales and the second are due to variations from external factors. A well-known internal variability is the occurrence of El Niño and La Niña. An example of a forced variation are the antrophogenic emissions of greenhouse gasses (GHG). The internal variability is also often called climate noise and the forced variability the climate signal. In the KNMI'23 scenarios the climate signal is quantified on the emissions based on the different Shared Socioeconomic Pathways (SSPs) used in the IPCC sixth assessment report (IPCC, 2021). Throughout this report the term SSPn-rf is used; where n is the number of the pathway and rf is the radiative forcing at the end of this century associated with the following pathways:

- SSP1: sustainability ('the green road')
- SSP2: the middle of the road
- SSP3: regional rivalry ('a rocky road')
- SSP4: inequality ('a divided road')
- SSP5: fossil-fuelled development ('taking the highway')

When deriving scenarios of future climate at a regional scale many uncertainties are present and different assumptions have to be made. For an upper and lower bound of projected global climate change (and associated global temperature change) the scenarios for sustainable development (SSP1-2.6) and the scenario for fossil-fuel intensive development (SSP5-8.5) are chosen. For these scenarios the median value of the IPCC range of climate sensitivity is chosen to determine the values of global temperature changes

within a SSP. Climate sensitivity is the magnitude of the global temperature change in response to a doubling of the CO2 concentration. Since the upper bound is not chosen, the radiative forcing associated with the SSP scenarios may also be reached with lower greenhouse gas emissions in combination with a high climate sensitivity. On top of these uncertainties the internal variability is introduced.

Hawkins and Sutton (2011) depict the different uncertainties very clear in Figure 1. In orange the internal variability of the climate system is depicted, in blue the model uncertainty related to the climate sensitivity present in different models, and in green the scenario uncertainty of the different SSPs.

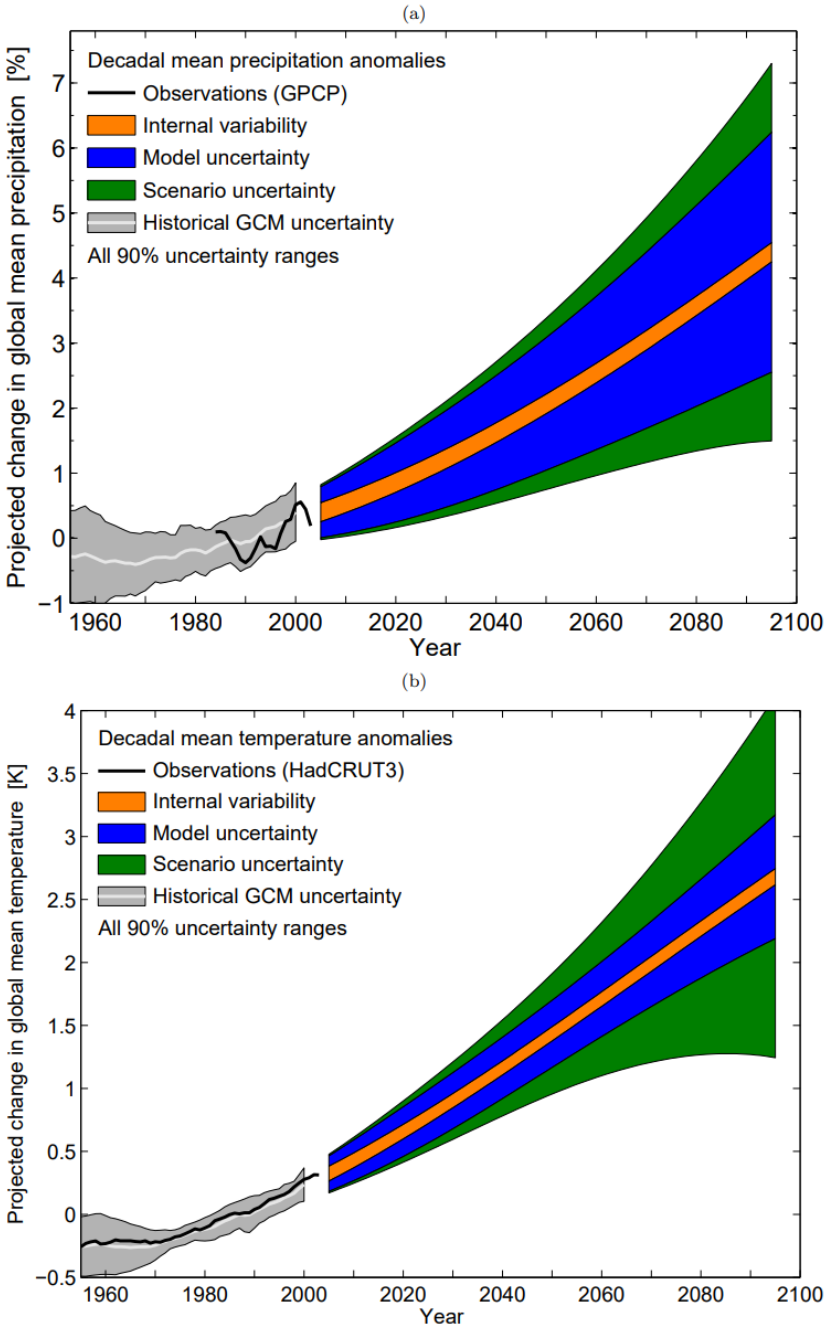

Figure 1: The total uncertainty in climate models separated into its three components: internal variability (orange), model uncertainty (blue) and scenario uncertainty (green) from Hawkins and Sutton (2011)

Next to the decision for two SSP scenarios, a storyline approach was taken to span the uncertainty in regional climate change conditional on a level of global climate change (warming level). The two storylines are selected to represent the range of precipitation changes projected by CMIP6 models for Suriname. This will result in four possible climate change scenarios (Figure 2). Storylines could have been developed for representing model uncertainty in temperature, radiation or wind, however the largest model uncertainty in future scenarios is seen for precipitation (Figure 1a). Next to that the amount of precipitation change in the future is very relevant for many sectors in Suriname and has a strong impact on future water availability and water safety.

These storylines are made up of the 10 most 'wetting' and the 10 most 'drying' models out of 29 CMIP6 models. To capture the changes in both the wet and dry season, group assignment was done based upon the changes in DJFM (Dec-Mar), AMJJ (Apr-Jul) and ASON (Aug-Nov) precipitation. This division follows Koole (2023), where the seasons are based upon months where it rains more than the mean annual precipitation (AMJJ), months where it rains less than the annual mean precipitation (ASON) and months where it rains in a similar amount as the mean annual precipitation (see Figure 3).

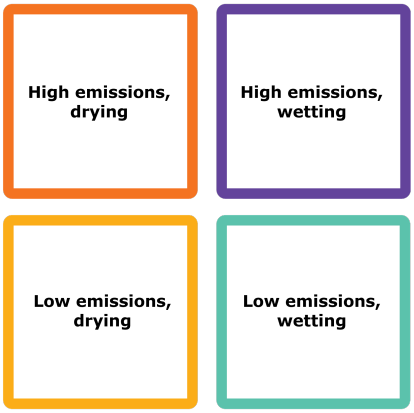

Figure 2: Four climate change scenario pathways following the KNMI'23 scenario's. (van Dorland et al., 2024)

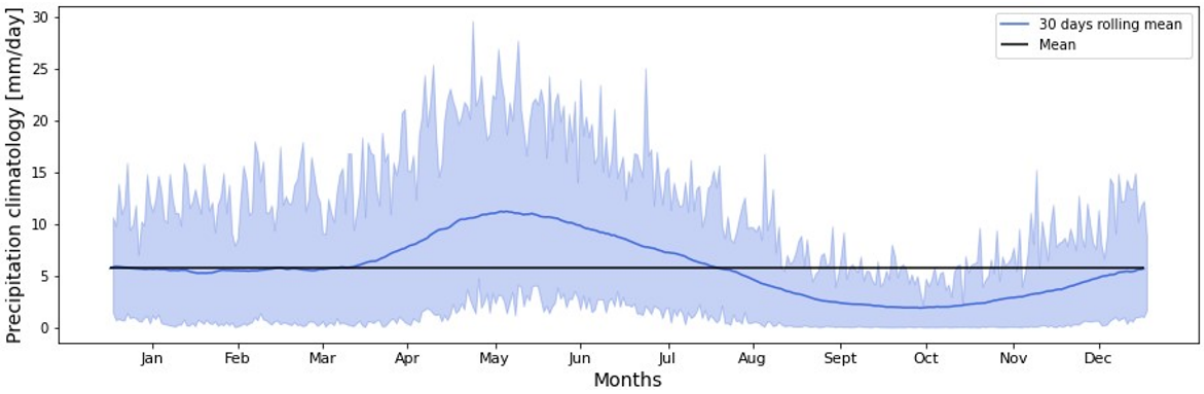

Figure 3: Climatology of the 30-day running mean precipitation [mm/day], for the period 1981-2020, averaged over Suriname. Including the band of precipitation between the 90th and 10th percentile. Data: GPCC Full Data Monthly Product Version 2020, 0.25° resolution Schneider et al. (2022).

The model output within these 4 scenario pathways is statistically downscaled to regional climate information. The global CMIP6 models are too coarse to provide detailed regional climate information and often have biases compared to the observational data. In Figure 4 on the left the raw CMIP6 output is shown for Suriname. The CMIP6 models show a large spread in the projected rainfall over Suriname, which means that there is a large uncertainty between the different models, confirming Figure 1a. On the right the regionally downscaled output is seen, which is bias adjusted, but still reveals a large uncertainty.

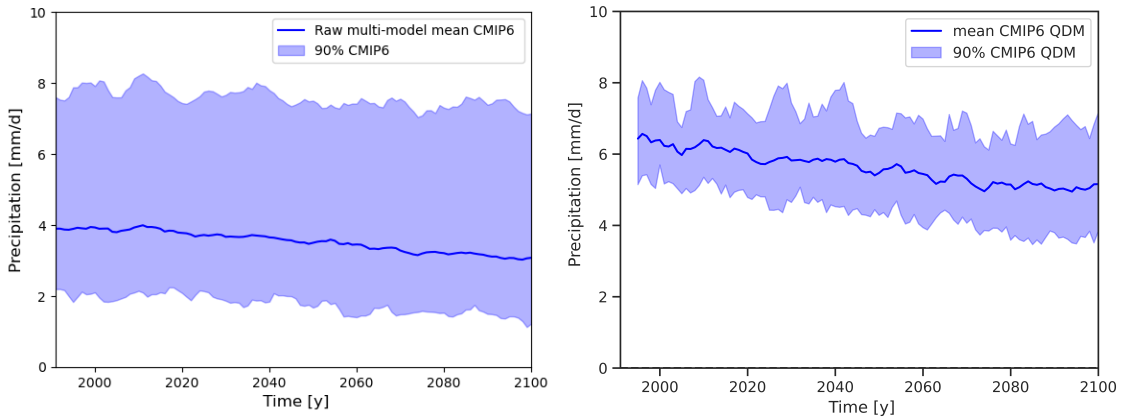

Figure 4: On the left the 5-year running mean raw multimodel mean CMIP6 data for Suriname [2N-6N and 51W-61.5W] and on the right the 5-year running mean downscaled (with Quantile Delta Mapping downscaling) CMIP6 data for station location Zanderij. Both graphs are based upon the SSP5-8.5 scenario.

This report continues with a summary of relevant findings from the latest IPCC report (IPCC, 2021) and the state of the climate report for Suriname (Solaun et al., 2021). Followed by a short oversight of current and historic trends for Suriname. This is followed by the construction and results of the KNMI Suriname scenarios.

2 Summary of IPCC on Northern South America (NSA) region

For comparison a summary of the results on Northern South America (NSA) from the International Panel on Climate Change (IPCC) Sixth Assessment Working Group I Report (AR6 WG I) (IPCC, 2021) are shown below.

Temperature: High confidence of increase of mean temperature and extreme heat.

Precipitation: There is medium confidence of projected decrease of mean precipitation. Medium confidence of increase in the intensity and frequency of heavy precipitation. Medium confidence in increase of aridity and agricultural and ecological drought. There are diverse historical precipitation trends in the region. Data scarcity persists for a representative assessment of heavy precipitation in the region.

Wind: Medium confidence of increase of mean windspeed and in wind power potential. Medium confidence of increase of tropical cyclones.

Sea level rise: High confidence of increase in relative sea level, coastal flooding, coastal erosion, marine heatwaves and ocean acidity. Around Central and South America, relative sea level has increased at a higher rate than the Global Mean Sea Level (GMSL) in the South Atlantic and the subtropical North Atlantic over the last 3 decades. Shoreline progradation rates have been observed in North-Western and Northern South America.

3 Summary of State of the climate report Suriname

For comparison a summary of the results from the State of the climate report Suriname (Solaun et al., 2021) are shown below. The State of the Climate Report Suriname is a study that has already looked at future climate change in Suriname by using climate models from CMIP6. However, only three climate models (HadGEM3-GC31, MIROC6 and IPSL-CM6A) were used in the State of the climate report, while 29 models are used within this study. The higher amount of models will give a large range of climate sensitivities and a more robust insight into climate projections.

Temperature: The annual mean, min and max temperatures are projected to increase. This increase is expected to be less pronounced at the coast and more pronounced in the southwest region of Suriname. Depending on the scenario, the mean temperature is projected to change from around 27°C to 29°C (+2°C - SSP2-4.5) or 31°C (+4°C - SSP5-8.5) by the end of the 21st century. Temperature extremes are projected to increase.

Precipitation: Precipitation is expected to decrease for all seasons, with precipitation episodes becoming rarer and more intense. By the end of the century strong reductions in annual precipitation by more than 20% for SSP5-8.5 are expected. The maximum precipitation for 1 and 5 days is expected to increase in the entire region.

Wind: There is low confidence that the average mean wind speed shows an increase in all scenarios. The number of days per year in which strong winds occur show very little change. Hurricanes in the Caribbean are expected to increase, but there is no evidence pointing to them affecting South America any more than they do now. Maximum windspeed is expected to increase moderately.

Sea level rise: The sea level anomaly will increase with a temperature increase and can be expected to surpass 0.25 meters by the end of the century for the high SSP5-8.5 scenario.

4 Observed local trends

To calculate long-term trends the ERA5 dataset (Hersbach et al., 2023) for temperature and the GPCC dataset (Schneider et al., 2022) for precipitation were used. For temperature there was no station data available for all of the four stations and therefore reanalysis data was chosen. To investigate a potential trend in the precipitation data, the GPCC dataset was chosen over station data, since this made it possible to investigate a longer time series. In Koole (2023) it was shown that when looking at monthly or annual values the GPCC dataset shows similar values as the station data.

In Figures 6 and 7 the annual mean values at the locations of the weather stations in Figure 5 are shown. The annual mean values where selected with the nearest gridpoint method. Over the annual values a trend was calculated making use of the standard KNMI trend calculation by de Valk (2020).

The yearly averaged temperature has increased with a rate of approximately 0.14 degree per decade since 1980 on the coast of Suriname and 0.13 degree per decade in the interior of Suriname. Precipitation measurements in Suriname show no significant trend.

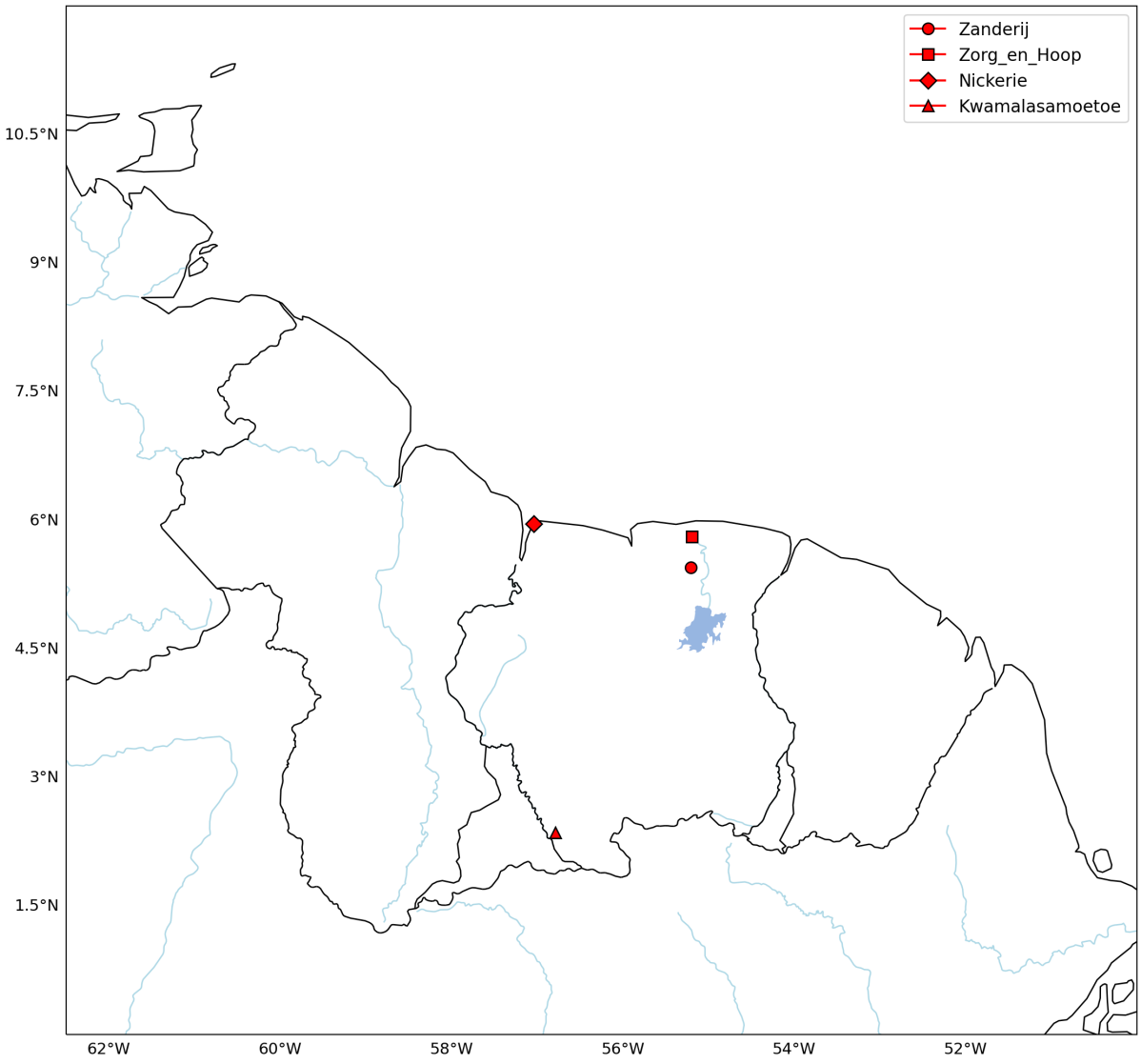

Figure 5: Location of stations that are used within this report.

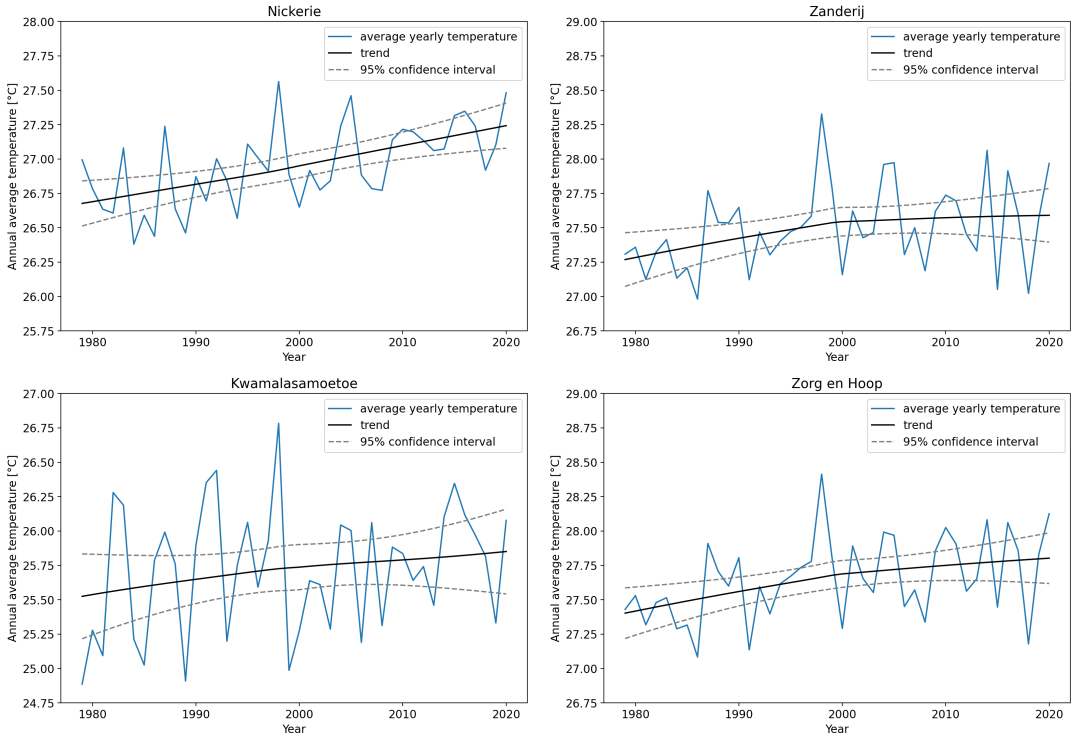

Figure 6: Annual average temperature since 1980, selected with the nearest gridpoint method at the location of the station in question. Note the different offset on the y-axis. Data: ERA5 reanalysis Hersbach et al. (2023). Trend calculation follows de Valk (2020)

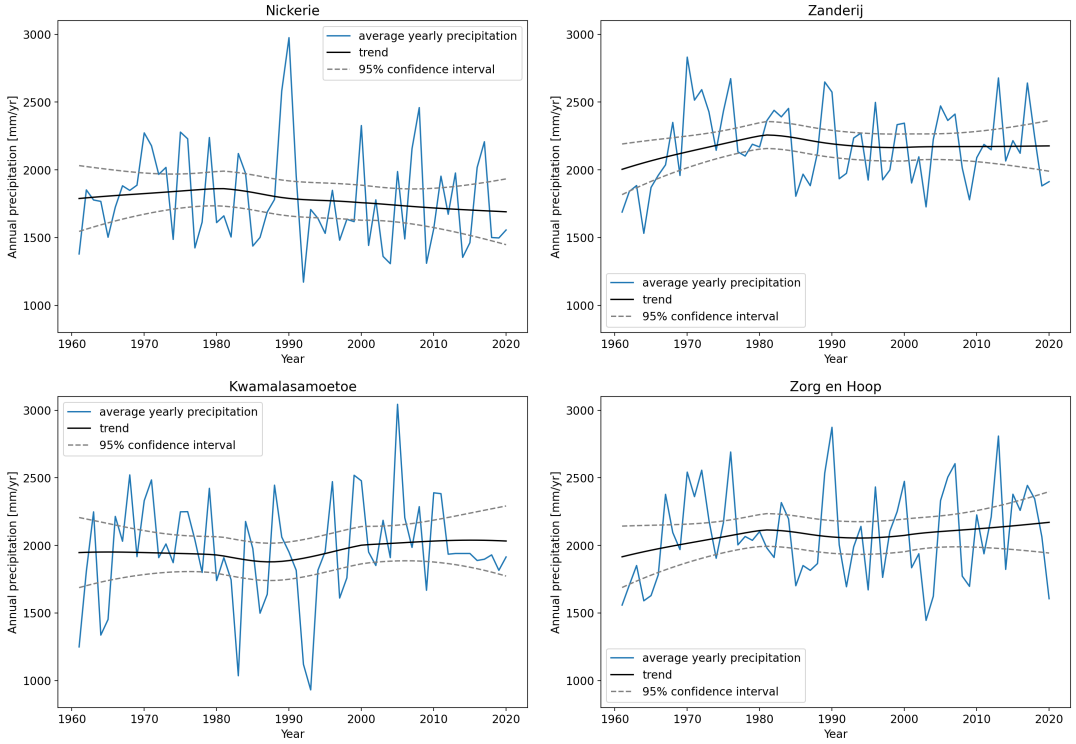

Figure 7: Annual precipitation amount, selected with the nearest gridpoint method at the location of the station in question. data: GPCC Full Data Monthly Product Version 2020, 0.25° Schneider et al. (2022). Trend calculation according to de Valk (2020)

5 Suriname scenarios for temperature, precipitation and wind

In this chapter the climate change scenarios for Suriname are discussed and explained for the variables of temperature, precipitation and wind. The focus lies on the expected mean changes within the different scenario pathways.

5.1 Data

Statistical downscaling (see Section 5.2) is done with daily precipitation data from station gauge data at the locations Zanderij, Zorg & Hoop, Nickerie and Kwamalasamoetoe. For the historical trend analysis the GPCC dataset was chosen over the station gauge data, however for the scenario analysis the daily precipitation values are needed. The GPCC data shows significantly less similarities with station gauge data for daily values than for monthly or annual values (Koole, 2023). Therefore station gauge data is chosen for the scenario development.

For the period 1991-2020 these station gauge observations have daily values with for most stations only a small number of missing data (0.9%, 1.4% and 0.4% for Zanderij, Zorg & Hoop and Nickerie, respectively). The station Kwamalasamoetoe is missing 15% of data in the period 1991-2020, but is still included to cover the interior part of Suriname. Caution should be taken when interpreting the results of the downscaling for Kwamalasamoetoe since a larger amount of missing observational data gives more uncertainties in the data after downscaling. Downscaling of temperature is done at the same locations with daily ERA5 t2m reanalysis data (Hersbach et al., 2023).

5.2 Methodology

The Suriname climate scenarios follow the same method that was used in the development of the scenarios for the Dutch Caribbean. In the KNMI'23 report the method of the climate scenarios is explained. The complete methodology can be viewed in van Dorland et al. (2024) and van der Wiel et al. (2024). For convenience the important steps of the methodology mentioned in Chapter 9 of van Dorland et al. (2024) are repeated here in this report:

1. **Selection of global temperature increase:** The change in global temperature (dTglob) for each forcing scenario and target year is selected based on the best estimate provided by IPCC AR6.

2. **Matched warming method:** The corresponding thirty-year period is selected for each CMIP6 model that reaches dTglob.

3. **Definition of model groups:** Two groups of models are defined based on the changes in dry season (ASON), wet season (AMJJ), and transitional season (DJFM) precipitation for Suriname by the end of the century under the SSP5-8.5 scenario.

4. **Statistical downscaling:** The CMIP6 models in each group undergo statistical downscaling using the Quantile Delta Mapping method. This process is applied to precipitation and temperature variables.

5. **Calculation of projected change:** The projected variables for the target years 2050 and 2100 are computed as a function of global warming using a smooth function to reduce the noise introduced by natural variability.

Step 1. Selection of global temperature increase

The scenarios have been developed for pre-selected SSP scenarios (see Chapter 1) that capture the uncertainty in future human emissions. For each of these SSP scenarios, the IPCC AR6 report provides projections of the Global Surface Air Temperature (GSAT). These GSATs are based on multiple lines of evidence regarding climate sensitivity to constrain the raw model projections. The IPCC refers to their constrained projections of global mean temperature change as the 'ΔGSAT assessed range'. Note that these projections thus differ from a straightforward CMIP6 multi-model mean, which would provide higher values for ΔGSAT (IPCC, 2021). The warming levels used in the KNMI'23 scenarios are based upon the ΔGSAT IPCC data. In Table 1 the warming levels (median values of the ΔGSAT assessed range) taken for each time horizon are shown. The time horizons are the 30 year periods around 2050 (2036-2065) and 2100 (2086-2115). The period 1991-2020 is the reference period for the present-day climate. For more detailed information the reader is referred to section 2.1.1 of van Dorland et al. (2024).

Emission uncertainty	Time horizons	
	2050	2100
SSP1-2.6	0.9 (0.5-1.3)	0.8 (0.4-1.5)
SSP2-4.5	1.1 (0.8-1.6)	1.9 (1.3-2.9)
SSP5-8.5	1.5 (1.0-2.0)	4.0 (2.8-5.6)

Table 1: KNMI'23 global warming levels, based on the the median value of the IPCC 'assessed range' of Global Surface Air Temperature change (ΔGSAT) relative to 1996-2015 [°C], for different SSP scenarios at the KNMI'23 time horizons, in brackets the 90% confidence interval (5-95 %).

Step 2. Matched warming method

Every CMIP6 model has a different climate sensitivity. Therefore, the time at which each model reaches the chosen warming levels is different. Highly sensitive models warm faster and reach the warming levels earlier in their simulation than low sensitivity models that warm relatively slow. In order to assess the projected regional climate change at the warming levels, each model is shifted in time such that the warming in that model matches the warming level of choice (Hausfather and Peters, 2020). This procedure is referred to as 'matched warming'.

Step 3. Definition of model groups

To define the two groups of models (the wet and dry group) the 1-dimensional area mean timeseries of the Suriname region is taken (defined as the region between 2N-6N and 51W-61.5W). After calculation of these timeseries the 10 driest models and the 10 wettest models are separated from the total amount of 29 CMIP6 models. This is done by ranking the models on the change in precipitation by 2100 for the AMJJ, ASON and DJFM season.

The selection of the model groups was conducted once, specifically for target year 2100 and SSP5-8.5, and subsequently applied to all other SSPs and target years (2050, 2100). This single-time model-grouping method, as opposed to creating wet/dry groups for each target year and SSP, reduces the noise introduced by internal variability and provides a better representation of the climate change signal in the projections.

Figure 8 shows the spread of the precipitation change (upper panel) and temperature change (lower panel) for the target year 2100 and the forcing scenario SSP5-8.5. The results are presented for the dry (red), wet (blue) and complete group of models (white). In the upper panel it is shown that the division into groups based upon the precipitation difference remains fairly consistent throughout the seasons, although the DJFM and ASON season show some overlap in precipitation change by the wet and dry group. The AMJJ season is most defined. From the lower panel it can be seen that there is a negative correlation between temperature and precipitation change; models with larger drying also project more temperature increase and vice versa. This relation will be discussed further in Chapter 5.5.

Important to remember is that these model groups do not capture the full range of model variability for temperature change, since the selection of the groups was done based upon precipitation change. It comes fairly close, because of the negative correlation between precipitation and temperatures. However, if temperature and precipitation changes were uncorrelated, basic statistical principles would suggest that both wet and dry groups would yield a temperature response close to the ensemble mean.

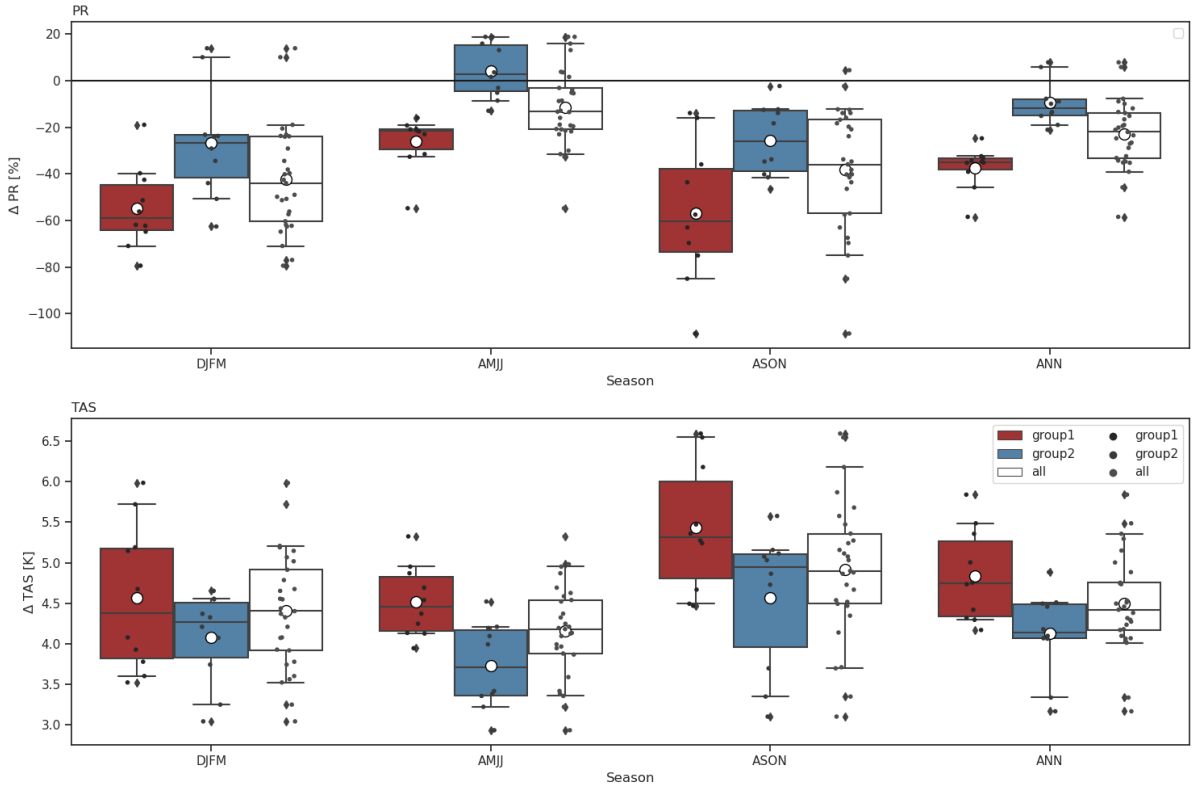

Figure 8: Spread of projected change in precipitation (upper panel) and temperature (lower panel) for the transitional season (DJFM), the long wet season (AMJJ), the long dry season (ASON) and annual period. Results are shown for the dry group of models (red), wet group of models (blue) and the entire set of models (white).

Step 4. Statistical downscaling

The fourth step of the methodology is the downscaling of the CMIP6 output to local variables. This is done by statistical downscaling instead of dynamical downscaling due to time and resource limitations. Only the raw CMIP6 data from temperature and precipitation are downscaled, not the wind data since not all CMIP6 models provide daily wind data output. The method used for the statistical downscaling of temperature and precipitation is the bias correction technique called Quantile Delta Mapping (QDM). More specifically the univariate QDM approach. Several studies (Dieng et al., 2022; Cannon et al., 2015) consider this approach suitable for correcting climate model output, particularly for precipitation. It is also employed by other meteorological institutes, such as MeteoSwiss (Feigenwinter et al., 2018).

QDM is a bias correction method that implicitly includes downscaling when the observed data set has a higher spatial resolution than the model grid. By comparing historical simulations with observations, QDM corrects systematic distributional biases in climate model outputs. To perform the QDM, the nearest grid point to the station location is selected for each CMIP6 model. The nearest grid point method is also employed in Feigenwinter et al., 2018. The QDM corrects systematic biases in the quantiles of a model. It achieves this by comparing quantiles of the present period's simulations with the quantiles derived from the observations (Feigenwinter et al., 2018; Cannon et al., 2015). QDM assumes that the biases in each quantile of the historical runs are the same for the future period. Therefore, the quantile trends are subtracted from the projected simulations, and the same quantile-dependent functions are applied. Finally, the quantile-dependent trends are added back to the corrected projected simulations. Consequently, QDM corrects the future projections while preserving the trend in each quantile (Cannon et al., 2015). Note that QDM does not preserve the mean trend itself. For a more comprehensive discussion of QDM, readers are referred to Section 2.1.10 in van Dorland et al. (2024).

For each location in Suriname the transformation functions are computed using 39 equally spaced quantiles ranging from 0 to 1. The transformation function is applied to the simulated time series using a moving window of thirty years. This approach ensures that the transformation function is consistently applied to thirty-year periods, which better represents extreme values. For temperature, the adjustment parameters in the transformation function are additive, while for precipitation they are multiplicative. In Figure 9 the cumulative distribution functions (CDFs) of temperature and precipitation for the observations (black line), the reference period simulations (blue line), and the future period simulations (with matched warming, red line) are shown for both the raw (continuous) and QDM corrected (dashed) time series. The CDFs for temperature (upper panels in Figure 9) exhibit a resemblance to a normal distribution, while the precipitation CDFs (lower panels in Figure 9) resemble an exponential distribution.

Step 5. Calculation of projected change

The last step of the production of the climate scenarios for Suriname is the computation of the projected change of the variables. This is done by expressing the projected variables as a function of global temperature change for each of the SSPs.

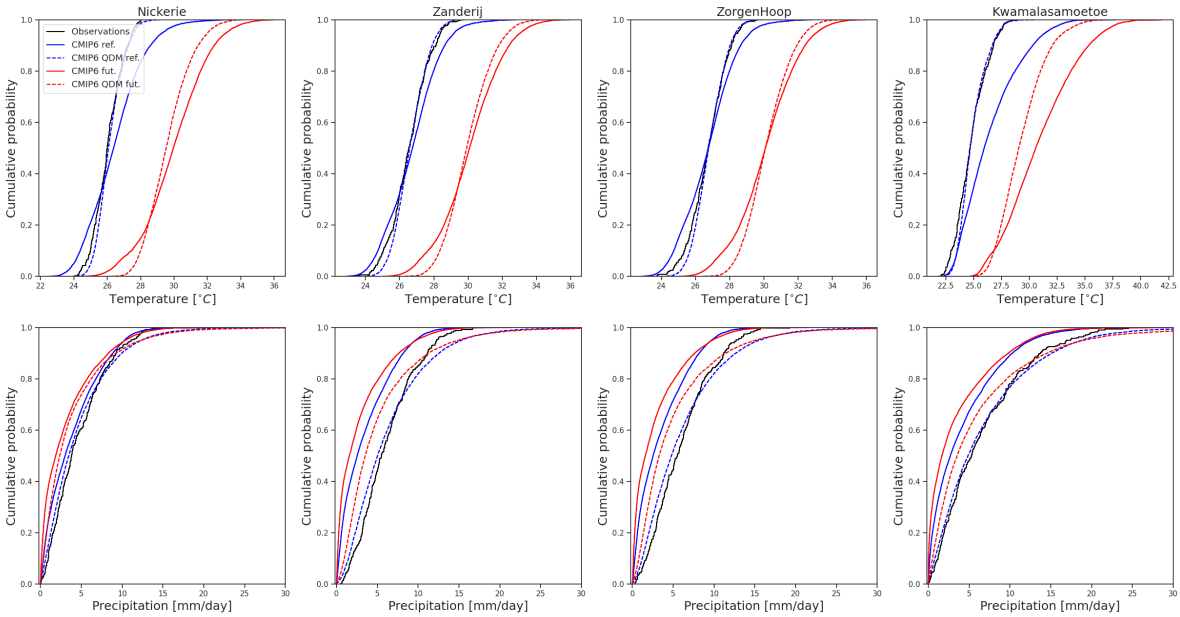

Figure 9: Cumulative distribution functions (CDFs) of temperature (upper panels) and precipitation (lower panels). The panels show results for the locations Nickerie, Zanderij, Zorg en Hoop and Kwamalasamoetoe. Black lines denote observations, blue lines CMIP6 model output (1991-2020) and red lines the future projections (matched warming, SSP5-8.5, 2100). Full lines show the raw (pre-QDM) CDF, dashed lines the corrected (post-QDM) CDF.

5.3 Projected local trends

The projected changes in annual mean temperature and precipitation for the locations Zanderij, Zorg & Hoop, Nickerie and Kwamalasamoetoe are depicted in Figure 10. Under the SSP1-2.6 forcing, the mean projected temperature change for Zanderij, Zorg & Hoop and Nickerie stays just under 1°C by 2100 and for Kwamalasamoetoe slightly over 1°C by 2100. Under the SSP5-8.5 forcing, the mean projected temperature increases continuously throughout the century up to a change of 4°C for Zanderij, Zorg & Hoop and Nickerie and an even bigger change of around 5°C for Kwamalasamoetoe (although with a larger uncertainty within the model group). The range of projected temperature change (90%-model spread, which includes interannual variability) across models is around ±1.5 °C.

The projected changes in annual mean precipitation span a much larger range of potential changes for the end of the century. The ensemble-mean change under SSP1-2.6 forcing is small. Under SSP5-8.5 forcing more precipitation changes are visible. The ensemble-mean change for 2100 lies around a 15-20% decrease in Zanderij, Zorg & Hoop en Nickerie, and a 10-15% decrease in Kwamalasamoetoe. However the range of projected precipitation change (90%-model spread, which includes interannual variability) across models is around 50%.

The projected changes in annual mean wind speed for Suriname, based upon the CMIP6 models (not statistically downscaled) are displayed in Figure 11. Under SSP1-2.6 forcing the multi-model shows no significant changes in wind speed for Zanderij, Zorg & Hoop and Nickerie. Kwamalasamoetoe shows a very small increase of around +1%. Under SSP5-8.5 forcing the multimodel mean shows a stronger increase for Nickerie and Kwamalasamoetoe

of respectively +2-3% and +4% by 2100.

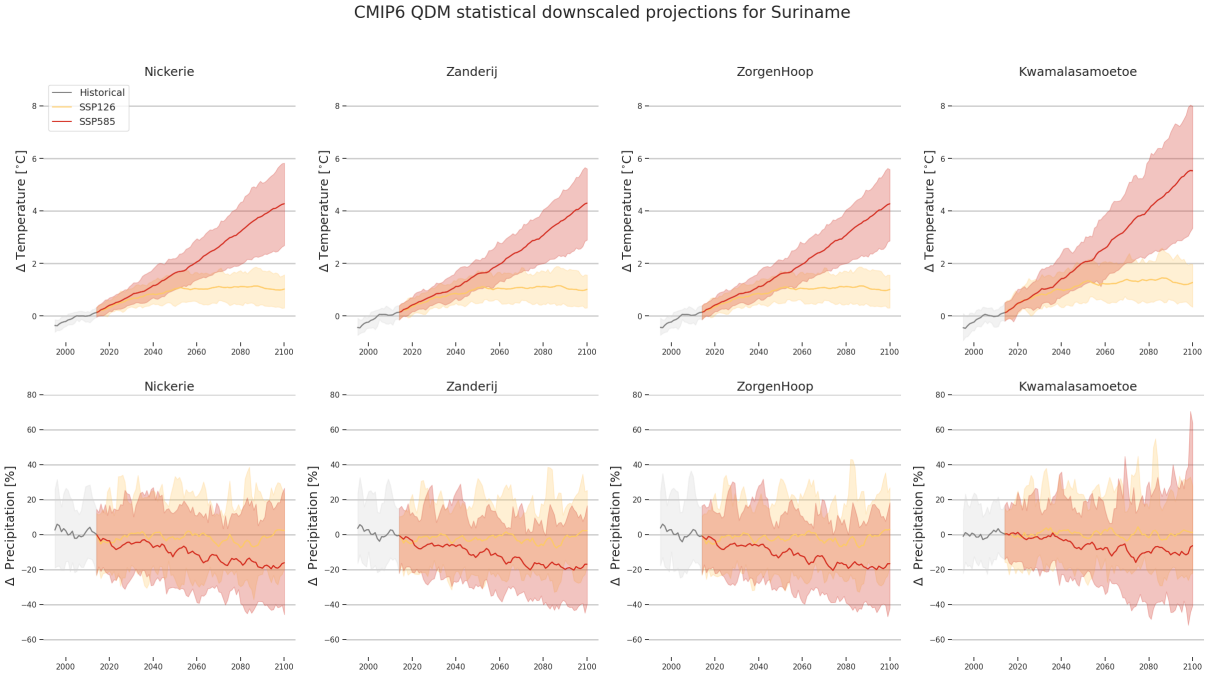

Figure 10: Projected changes in 5-year running annual-mean temperature (upper panel) and precipitation (lower panel) Nickerie, Zanderij, Zorg & Hoop and Kwamalasamoetoe. The time series shown are the 29 CMIP6 models statistically downscaled and forced by SSP1-2.6 (yellow) and SSP5-8.5 (red). The historical period is shown in grey. The thick lines show the multi-model mean while the shaded regions show the 90% spread.

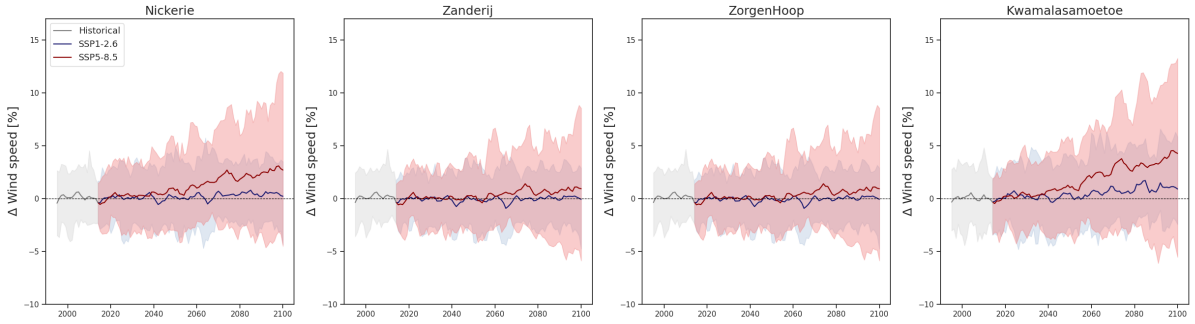

Figure 11: Projected change in wind speed Nickerie, Zanderij, Zorg & Hoop and Kwamalasamoetoe. The time series shown are for the 29 CMIP6 models (not statistically downscaled) forced by SSP1-2.6 (blue) and SSP5-8.5 (red). The historical period is shown in grey. The thick lines show the multimodel mean, while the shaded regions show the 90% spread.

Season	Variable	Indicator	1991-2020 observations	2050 ssp126 dry trend	2050 ssp126 wet trend	2050 ssp245K dry trend	2050 ssp245K wet trend	2050 ssp585K dry trend	2050 ssp585K wet trend	2100 ssp126K dry trend	2100 ssp126K wet trend	2100 ssp245K dry trend	2100 ssp245K wet trend	2100 ssp585K dry trend	2100 ssp585K wet trend
Annual	Temperature	average	26.6 °C	0.9 °C	0.9 °C	1.1 °C	1.1 °C	1.5 °C	1.4 °C	0.8 °C	0.8 °C	1.9 °C	1.8 °C	3.9 °C	3.8 °C
		year-to-year variations	0.3 °C	0.0 °C	0.0 °C	0.1 °C	0.0 °C	0.1 °C	0.1 °C	0.0 °C	0.0 °C	0.1 °C	0.1 °C	0.2 °C	0.2 °C
	Precipitation	average amount	2172.5 mm	-9.3%	-3.2%	-11.1%	-3.8%	-14.6%	-4.9%	-8.3%	-2.9%	-17.8%	-5.9%	-33.3%	-8.5%
		year-to-year variations	251.8 mm	-1.9%	2.4%	-2.6%	3.3%	-4.0%	5.3%	-1.6%	2.0%	-5.6%	7.5%	-12.1%	18.3%
DJFM_season	Temperature	average	25.9 °C	0.9 °C	0.8 °C	1.1 °C	1.0 °C	1.5 °C	1.4 °C	0.8 °C	0.7 °C	1.9 °C	1.8 °C	3.8 °C	3.7 °C
	Precipitation	average amount	623.9 mm	-13.7%	-8.1%	-16.3%	-9.8%	-21.1%	-13.0%	-12.3%	-7.3%	-25.5%	-15.9%	-45.6%	-28.6%
AMJJ_season	Temperature	average	26.4 °C	0.8 °C	0.8 °C	1.0 °C	1.0 °C	1.4 °C	1.4 °C	0.7 °C	0.8 °C	1.8 °C	1.8 °C	3.9 °C	3.7 °C
	Precipitation	average amount	1062.5 mm	-5.0%	0.6%	-6.1%	0.7%	-8.3%	1.1%	-4.4%	0.5%	-10.4%	1.5%	-21.4%	6.1%
ASON_season	Temperature	average	27.4 °C	1.0 °C	0.9 °C	1.2 °C	1.1 °C	1.7 °C	1.5 °C	0.9 °C	0.8 °C	2.1 °C	1.9 °C	4.2 °C	4.1 °C
	Precipitation	average amount	465.4 mm	-12.3%	-5.3%	-14.6%	-6.3%	-18.8%	-7.9%	-11.1%	-4.8%	-22.7%	-9.4%	-41.9%	-15.2%

Season	Variable	Indicator	1991-2020 observations	2050 ssp126 dry trend	2050 ssp126 wet trend	2050 ssp245K dry trend	2050 ssp245K wet trend	2050 ssp585K dry trend	2050 ssp585K wet trend	2100 ssp126K dry trend	2100 ssp126K wet trend	2100 ssp245K dry trend	2100 ssp245K wet trend	2100 ssp585K dry trend	2100 ssp585K wet trend
Annual	Wind	average wind speed	2.5m/s	0.4%	-0.4%	0.5%	-0.4%	0.7%	-0.4%	0.3%	-0.4%	0.9%	-0.4%	2.1%	-0.4%
		year-to-year variations	0.3m/s	-4.1%	1.0%	-5.0%	1.3%	-6.5%	1.7%	-3.7%	0.9%	-7.8%	2.0%	-12.2%	2.2%
DJFM_season	Wind	average	2.7m/s	-0.4%	-0.4%	-0.5%	-0.4%	-0.8%	-0.5%	-0.4%	-0.3%	-1.0%	-0.6%	-2.1%	-1.2%
AMJJ_season	Wind	average	2.3m/s	-0.3%	-1.2%	-0.3%	-1.3%	-0.3%	-1.7%	-0.2%	-1.1%	-0.2%	-1.9%	0.5%	-3.0%
ASON_season	Wind	average	2.6m/s	2.0%	0.4%	2.5%	0.6%	3.4%	0.9%	1.8%	0.4%	4.2%	1.3%	8.7%	3.2%

Figure 12: Climate scenarios for Zanderij. The variables are evaluated for the entire year (annual) as well as for the wet season (AMJJ), the dry season (ASON) and the transitional season (DJFM). Interannual variability is calculated on a yearly basis.

			1991-2020 observations	2050 ssp126 dry trend	2050 ssp126 wet trend	2050 ssp245K dry trend	2050 ssp245K wet trend	2050 ssp585K dry trend	2050 ssp585K wet trend	2100 ssp126K dry trend	2100 ssp126K wet trend	2100 ssp245K dry trend	2100 ssp245K wet trend	2100 ssp585K dry trend	2100 ssp585K wet trend
Season	*Variable*	*Indicator*													
Annual	Temperature	average	26.7 °C	0.9 °C	0.9 °C	1.1 °C	1.1 °C	1.5 °C	1.4 °C	0.8 °C	0.8 °C	1.9 °C	1.8 °C	3.9 °C	3.8 °C
		year-to-year variations	0.3 °C	0.0 °C	0.0 °C	0.0 °C	0.0 °C	0.1 °C	0.1 °C	0.0 °C	0.0 °C	0.1 °C	0.1 °C	0.2 °C	0.2 °C
	Precipitation	average amount	2151.9 mm	-9.1%	-3.1%	-10.9%	-3.7%	-14.4%	-4.7%	-8.2%	-2.8%	-17.6%	-5.6%	-33.2%	-8.2%
		year-to-year variations	298.3 mm	-1.6%	2.5%	-2.2%	3.4%	-3.6%	5.5%	-1.4%	2.1%	-5.0%	7.8%	-11.2%	17.9%
DJFM_season	Temperature	average	26.1 °C	0.9 °C	0.8 °C	1.1 °C	1.0 °C	1.5 °C	1.4 °C	0.8 °C	0.7 °C	1.9 °C	1.8 °C	3.8 °C	3.7 °C
	Precipitation	average amount	606.0 mm	-13.9%	-8.3%	-16.5%	-10.0%	-21.5%	-13.3%	-12.5%	-7.5%	-26.0%	-16.3%	-47.1%	-29.3%
AMJJ_season	Temperature	average	26.6 °C	0.8 °C	0.8 °C	1.0 °C	1.0 °C	1.4 °C	1.4 °C	0.7 °C	0.8 °C	1.8 °C	1.8 °C	3.9 °C	3.7 °C
	Precipitation	average amount	1069.4 mm	-4.6%	0.7%	-5.7%	0.9%	-7.8%	1.3%	-4.1%	0.7%	-9.9%	1.8%	-20.5%	6.4%
ASON_season	Temperature	average	27.4 °C	1.0 °C	0.9 °C	1.2 °C	1.1 °C	1.6 °C	1.5 °C	0.9 °C	0.8 °C	2.1 °C	1.9 °C	4.2 °C	4.1 °C
	Precipitation	average amount	456.3 mm	-12.2%	-5.1%	-14.5%	-6.0%	-18.8%	-7.6%	-11.0%	-4.6%	-22.8%	-9.0%	-42.2%	-14.8%

			1991-2020 observations	2050 ssp126 dry trend	2050 ssp126 wet trend	2050 ssp245K dry trend	2050 ssp245K wet trend	2050 ssp585K dry trend	2050 ssp585K wet trend	2100 ssp126K dry trend	2100 ssp126K wet trend	2100 ssp245K dry trend	2100 ssp245K wet trend	2100 ssp585K dry trend	2100 ssp585K wet trend
Season	*Variable*	*Indicator*													
Annual	Wind	average wind speed	2.9m/s	0.4%	-0.4%	0.5%	-0.4%	0.7%	-0.4%	0.3%	-0.4%	0.9%	-0.4%	2.1%	-0.4%
		year-to-year variations	0.3m/s	-4.1%	1.0%	-5.0%	1.3%	-6.5%	1.7%	-3.7%	0.9%	-7.8%	2.0%	-12.2%	2.2%
DJFM_season	Wind	average	3.3m/s	-0.4%	-0.4%	-0.5%	-0.4%	-0.8%	-0.5%	-0.4%	-0.3%	-1.0%	-0.6%	-2.1%	-1.2%
AMJJ_season	Wind	average	2.6m/s	-0.3%	-1.2%	-0.3%	-1.3%	-0.3%	-1.7%	-0.2%	-1.1%	-0.2%	-1.9%	0.5%	-3.0%
ASON_season	Wind	average	2.8m/s	2.0%	0.4%	2.5%	0.6%	3.4%	0.9%	1.8%	0.4%	4.2%	1.3%	8.7%	3.2%

Figure 13: Climate scenarios for Zorg en Hoop. The variables are evaluated for the entire year (annual) as well as for the wet season (AMJJ), the dry season (ASON) and the transitional season (DJFM). Interannual variability is calculated on a yearly basis.

Season	Variable	Indicator	1991_2020 observations	2050 ssp126 dry trend	2050 ssp126 wet trend	2050 ssp245K dry trend	2050 ssp245K wet trend	2050 ssp585K dry trend	2050 ssp585K wet trend	2100 ssp126K dry trend	2100 ssp126K wet trend	2100 ssp245K dry trend	2100 ssp245K wet trend	2100 ssp585K dry trend	2100 ssp585K wet trend
Annual	Temperature	average	26.0 °C	0.9 °C	0.9 °C	1.1 °C	1.0 °C	1.6 °C	1.4 °C	0.8 °C	0.8 °C	2.0 °C	1.8 °C	4.1 °C	3.9 °C
		year-to-year variations	0.2 °C	0.1 °C	0.0 °C	0.1 °C	0.1 °C	0.2 °C	0.1 °C	0.1 °C	0.0 °C	0.2 °C	0.1 °C	0.3 °C	0.3 °C
	Precipitation	average amount	1667.9 mm	-8.0%	-1.8%	-9.6%	-2.2%	-12.5%	-2.8%	-7.2%	-1.6%	-15.3%	-3.3%	-29.1%	-4.0%
		year-to-year variations	342.2 mm	-0.2%	3.1%	-0.4%	4.2%	-0.9%	6.7%	-0.1%	2.6%	-1.5%	9.5%	-5.3%	22.9%
DJFM_season	Temperature	average	25.6 °C	0.9 °C	0.8 °C	1.1 °C	1.0 °C	1.5 °C	1.4 °C	0.8 °C	0.7 °C	1.9 °C	1.8 °C	3.9 °C	3.8 °C
	Precipitation	average amount	477.6 mm	-12.5%	-7.9%	-14.9%	-9.6%	-19.5%	-12.8%	-11.2%	-7.1%	-23.7%	-15.8%	-43.9%	-29.2%
AMJJ_season	Temperature	average	25.8 °C	0.8 °C	0.8 °C	1.0 °C	1.0 °C	1.4 °C	1.4 °C	0.7 °C	0.7 °C	1.8 °C	1.7 °C	3.9 °C	3.7 °C
	Precipitation	average amount	857.0 mm	-3.9%	1.7%	-4.7%	2.2%	-6.3%	3.0%	-3.5%	1.5%	-7.8%	4.0%	-15.6%	11.3%
ASON_season	Temperature	average	26.7 °C	1.1 °C	0.9 °C	1.3 °C	1.1 °C	1.7 °C	1.5 °C	0.9 °C	0.8 °C	2.2 °C	1.9 °C	4.4 °C	4.1 °C
	Precipitation	average amount	317.5 mm	-11.0%	-2.2%	-13.2%	-2.7%	-17.4%	-3.7%	-9.9%	-2.0%	-21.3%	-4.6%	-41.9%	-10.0%

Season	Variable	Indicator	1991_2020 observations	2050 ssp126 dry trend	2050 ssp126 wet trend	2050 ssp245K dry trend	2050 ssp245K wet trend	2050 ssp585K dry trend	2050 ssp585K wet trend	2100 ssp126K dry trend	2100 ssp126K wet trend	2100 ssp245K dry trend	2100 ssp245K wet trend	2100 ssp585K dry trend	2100 ssp585K wet trend
Annual	Wind	average wind speed	4.6m/s	0.7%	-0.3%	0.9%	-0.3%	1.3%	-0.2%	0.6%	-0.3%	1.7%	-0.1%	4.1%	0.7%
		year-to-year variations	0.4m/s	-4.5%	1.1%	-5.5%	1.2%	-7.7%	1.5%	-3.9%	1.0%	-9.9%	1.6%	-18.2%	0.6%
DJFM_season	Wind	average	5.4m/s	-0.2%	-0.2%	-0.3%	-0.3%	-0.4%	-0.3%	-0.2%	-0.2%	-0.5%	-0.3%	-1.2%	-0.6%
AMJJ_season	Wind	average	4.2m/s	0.4%	-0.7%	0.5%	-0.8%	0.8%	-0.9%	0.3%	-0.7%	1.2%	-1.0%	3.3%	-1.0%
ASON_season	Wind	average	4.2m/s	2.3%	0.2%	2.8%	0.4%	4.0%	0.8%	2.0%	0.1%	5.1%	1.3%	11.4%	4.4%

Figure 14: Climate scenarios for Nickerie. The variables are evaluated for the entire year (annual) as well as for the wet season (AMJJ), the dry season (ASON) and the transitional season (DJFM). Interannual variability is calculated on a yearly basis.

			1991-2020 observations	2050 ssp126 dry trend	2050 ssp126 wet trend	2050 ssp245K dry trend	2050 ssp245K wet trend	2050 ssp585K dry trend	2050 ssp585K wet trend	2100 ssp126K dry trend	2100 ssp126K wet trend	2100 ssp245K dry trend	2100 ssp245K wet trend	2100 ssp585K dry trend	2100 ssp585K wet trend
Season	*Variable*	*Indicator*													
Annual	Temperature	average	24.8 °C	1.2 °C	1.0 °C	1.5 °C	1.2 °C	2.1 °C	1.6 °C	1.1 °C	0.9 °C	2.6 °C	2.1 °C	5.5 °C	4.6 °C
		year-to-year variations	0.4 °C	0.2 °C	0.1 °C	0.3 °C	0.1 °C	0.3 °C	0.2 °C	0.2 °C	0.1 °C	0.4 °C	0.2 °C	0.6 °C	0.5 °C
	Precipitation	average amount	1992.7 mm	-6.3%	1.5%	-7.6%	1.7%	-10.1%	2.0%	-5.6%	1.4%	-12.5%	2.3%	-24.0%	5.0%
		year-to-year variations	740.0 mm	-0.2%	5.4%	-0.3%	7.1%	-0.7%	11.1%	-0.1%	4.6%	-1.1%	15.4%	-3.6%	34.6%
DJFM_season	Temperature	average	24.3 °C	1.2 °C	1.0 °C	1.5 °C	1.2 °C	2.0 °C	1.6 °C	1.1 °C	0.8 °C	2.5 °C	2.1 °C	5.1 °C	4.6 °C
	Precipitation	average amount	517.5 mm	-8.5%	-3.6%	-10.3%	-4.5%	-13.7%	-6.3%	-7.6%	-3.1%	-17.0%	-8.0%	-32.3%	-14.4%
AMJJ_season	Temperature	average	24.3 °C	1.1 °C	0.9 °C	1.3 °C	1.1 °C	1.8 °C	1.5 °C	0.9 °C	0.8 °C	2.3 °C	1.9 °C	5.0 °C	4.2 °C
	Precipitation	average amount	1155.2 mm	-3.8%	4.8%	-4.6%	5.7%	-5.9%	7.5%	-3.5%	4.3%	-7.2%	9.2%	-13.1%	19.6%
ASON_season	Temperature	average	25.8 °C	1.4 °C	1.0 °C	1.8 °C	1.3 °C	2.4 °C	1.8 °C	1.3 °C	0.9 °C	3.1 °C	2.3 °C	6.5 °C	5.2 °C
	Precipitation	average amount	302.7 mm	-10.1%	-2.3%	-12.4%	-3.1%	-17.2%	-5.0%	-8.9%	-1.9%	-22.0%	-7.1%	-47.4%	-19.2%

			1991-2020 observations	2050 ssp126 dry trend	2050 ssp126 wet trend	2050 ssp245K dry trend	2050 ssp245K wet trend	2050 ssp585K dry trend	2050 ssp585K wet trend	2100 ssp126K dry trend	2100 ssp126K wet trend	2100 ssp245K dry trend	2100 ssp245K wet trend	2100 ssp585K dry trend	2100 ssp585K wet trend
Season	*Variable*	*Indicator*													
Annual	Wind	average wind speed	2.0m/s	1.0%	-0.4%	1.2%	-0.3%	1.9%	-0.2%	0.8%	-0.4%	2.5%	-0.0%	6.4%	1.3%
		year-to-year variations	0.3m/s	-3.9%	1.2%	-4.9%	1.4%	-6.7%	1.4%	-3.5%	1.2%	-8.6%	1.3%	-16.2%	-1.4%
DJFM_season	Wind	average	2.7m/s	-0.4%	-0.3%	-0.4%	-0.3%	-0.4%	-0.3%	-0.3%	-0.3%	-0.4%	-0.3%	-0.1%	-0.1%
AMJJ_season	Wind	average	1.6m/s	1.3%	-0.6%	1.6%	-0.6%	2.3%	-0.5%	1.1%	-0.5%	3.0%	-0.4%	6.9%	0.7%
ASON_season	Wind	average	1.7m/s	2.5%	-0.1%	3.2%	-0.0%	4.7%	0.3%	2.2%	-0.2%	6.3%	0.8%	15.4%	4.0%

Figure 15: Climate scenarios for Kwamalasamoetoe. The variables are evaluated for the entire year (annual) as well as for the wet season (AMJJ), the dry season (ASON) and the transitional season (DJFM). Interannual variability is calculated on a yearly basis.

5.4 Scenario tables for Suriname

As seen in the previous section, the projections for Suriname give a broad range of possible future values for temperature, precipitation and wind. This results both from model spread and natural interannual variability. In the Tables 12,13,14 and 15 climate scenarios for the target years 2050 and 2100 are presented. This is done using the methods described in section 5.2; for each emission pathway a dry-trending and wet-trending scenario is created by using the 30 year period around the target year. The final result in Tables 12-15 consist of tables of estimated mean changes and interannual variability. Scenario values are produced for the four station locations Zanderij, Zorg & Hoop, Nickerie and Kwamalasamoetoe and for the annual mean, the dry season (ASON), the wet season (AMJJ) and the transitional season (DJFM).

A few notable observations can be drawn from these tables. The warming continues throughout both the wet-trending and the dry-trending high emission scenarios (Hn, and Hd respectively). The largest temperature increase is expected for the dry (ASON) season. Where the wet-trending and dry-trending scenarios show a similar temperature increase for the locations Zanderij, Zorg & Hoop and Nickerie, the expected increase in temperature for the location Kwamalasamoetoe varies almost 1 degree between the two pathways. With a possibility of a +6.5 degrees increase in temperature in the dry (ASON) season in the dry-trending scenario. In the low emission scenarios (Ln, and Ld) the warming plateaus around +1 degrees for the target year 2050 and remains approximately constant towards target year 2100. The largest differences in temperature are therefore caused by the emission pathways.

For precipitation the largest differences are seen between the dry-trending and wet-trending scenarios instead of between the emission pathways. The coastal locations Zanderij, Zorg & Hoop and Nickerie show a different pattern from the location of Kwamalasamoetoe more inland, therefore both will be discussed separately.

On the coast, annual reductions of around 30% are seen for the Hd scenario for target year 2100, and much smaller reductions of 4-8% for the Hn scenario. Only the wet (AMJJ) season shows an increase in mean precipitation between 6-11% for the Hn scenario towards target year 2100. However still a decrease in precipitation for the Hd scenario. The change in precipitation during the wet (AMJJ) season is therefore dependent on the storyline that is chosen. The low emission pathways show relatively small changes in precipitation compared to the broad range in future values.

For the inland location of Kwamalasamoetoe, annual reductions of around 24% are seen for the Hd scenario for target year 2100, and a small increase of 5% for the Hn scenario. There are significant differences between the projections for the dry (ASON) and the wet (AMJJ) season. Both Hd and Hn scenario expect a strong decrease in mean precipitation in the dry (ASON) season of 47% and 19% respectively. In the wet (AMJJ) season the Hd scenario projects a decrease of 13% compared to an increase of 20% in mean precipitation for the Hn scenario.

At last, for wind speed, the changes are not that defined. The maximal increase in annual wind speed occurring under Hd for target year 2100 are between 2 and 6%. Interesting is that all locations show the largest increase in wind in the ASON season (9-15%) and a small decrease of about 1% in wind in the DJFM season. The changes for the low emission scenarios are even smaller.

In general the scenario numbers presented in Tables 12, 13, 14 and 15 span a smaller width

than the CMIP6 model plumes seen in Figures 10 and 11. Since the scenario pathways are based upon wetting and drying CMIP6 models the scenario numbers for precipitation are close to spanning the entire width of the CMIP6 plumes. The temperature and wind scenario numbers lay closer to the ensemble mean signals of the CMIP6 SSP pathways.

5.5 Influence of ENSO and AMOC on climate scenarios Suriname

For insight into the large scale drivers behind the climate change scenarios in Suriname it is important to look at the spatial pattern in precipitation, temperature and wind changes for a larger area. Figures 16-17 show the ensemble-mean projected change for the dry and wet groups at the end of the century under SSP5-8.5. This scenario was selected due to its higher signal-to-noise ratio, enabling the identification of distinct atmospheric processes.

The expected temperature change for Suriname is consistent with the changes expected for the rest of Northern South-America, where the strongest changes are expected in the interior of the continent, especially in the months August-November, as seen in Figure 16. Some clear visible patterns of warming are the east equatorial warming over the Pacific ocean and the Pacific warming around 20-30°N.

The first thing that becomes visible in Figure 17 is that the precipitation changes for Suriname are consistent within the larger area around Suriname. In addition, various larger regions with distinct increases in precipitation and other regions with distinct decreases in precipitation are visible. One of the things that stands out is the dipole pattern of precipitation change. Especially in the dry group, there is a strong increase in precipitation visible over the Pacific around the equator and a strong decrease of precipitation more eastward over Northern South America. Understanding these apparent patterns in precipitation change helps to define the mechanisms behind the expected changes in precipitation for Suriname.

The main processes now responsible for natural variability in precipitation amount over Suriname are the El Niño Southern Oscillation (ENSO) and the meridional amplitude and intensity of the Inter Tropical Convergence Zone (ITCZ) (Córdova et al., 2022; Cai et al., 2020; Bovolo, 2010). The El Niño Southern Oscillation (ENSO) is a coupled ocean-atmosphere phenomenon, where the Pacific sea surface temperatures (SSTs) are coupled to the Walker circulation. The El Niño phase of ENSO is characterized by anomalously warm east-equatorial Pacific SSTs, which drives an eastward migration of the Walker circulation. This in its turn results in subsidence over Suriname, resulting in warmer and drier conditions. In reverse, the La Niña phase of ENSO presents with colder east-equatorial Pacific SSTs, a westward migration of the Walker circulation and colder and wetter conditions over Suriname (McPhaden et al., 2020).

Overall CMIP6 models show a dominant El Niño-like circulation (or eastward migration of the Walker circulation) due to global warming (Fredriksen et al., 2020; Seager et al., 2021; Brotons et al., 2024). This is supported by the east-equatorial warming of the Pacific ocean (visible in Figure 16). Next to that, there is a strong increase in precipitation over the Pacific equatorial region. Over the equatorial Atlantic the precipitation increase is weaker, with a decrease in precipitation over the subtropical Atlantic regions. All this is coherent with an increase in El Niño conditions.

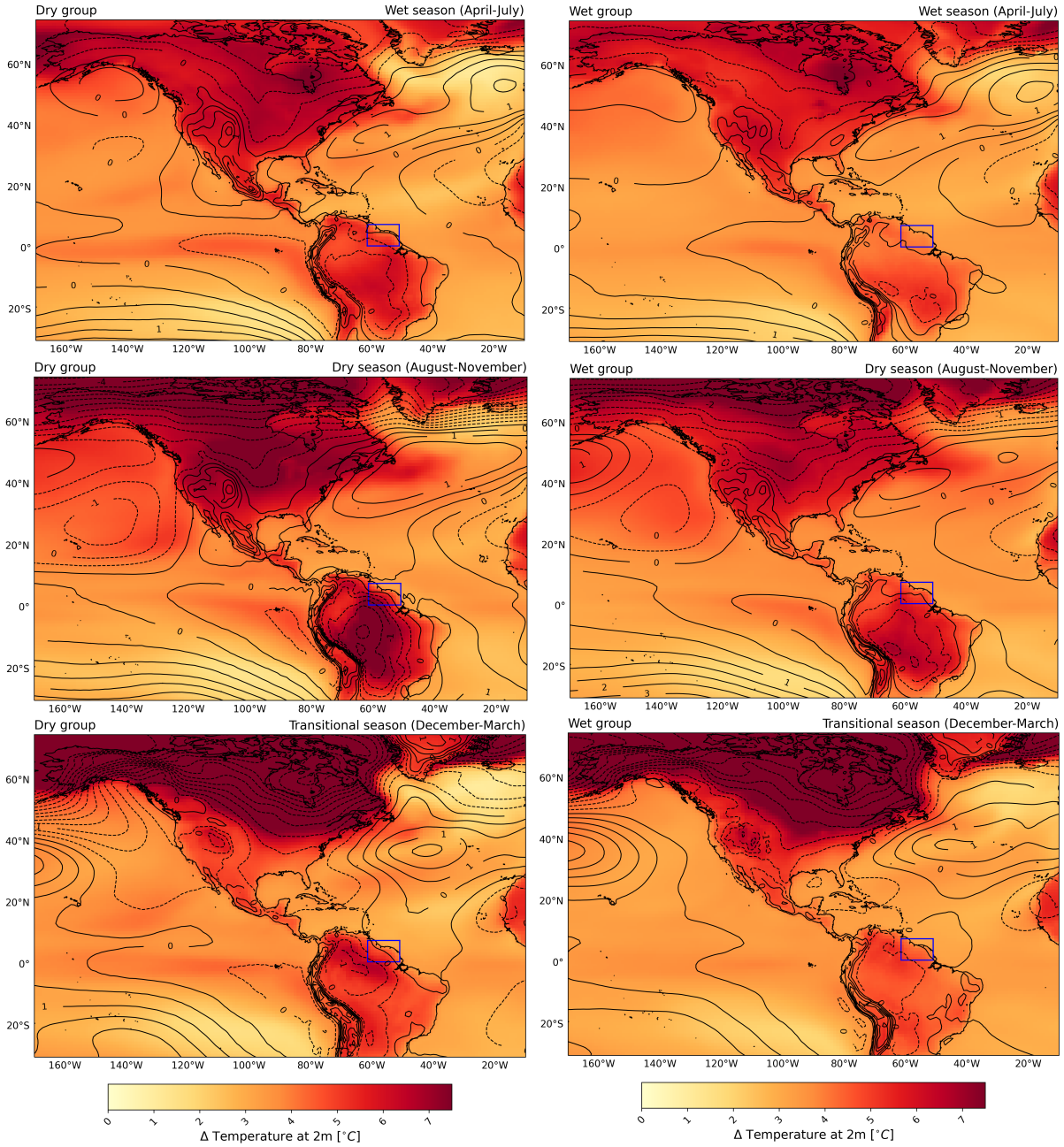

Figure 16: Projected change in 2m-temperature (colors, in °C) and sea level pressure (contours, in hPa) for the dry (left panels) and wet (right panels) groups of models under SSP5-8.5 in 2100 (matched warming). Positive sea level pressure changes are represented by continuous lines, negative changes are dashed. Changes are shown for the AMJJ, ASON and DJFM seasons in the upper, middle and lower panels, respectively. The figures show the raw (i.e., not downscaled) multimodel mean of the 10 CMIP6 models in each group. The blue box indicates the Guyanas region.

El Niño like conditions seem to be more pronounced in the dry model group compared to the wet model group. The dry groups show stronger warming over the eastern Pacific and the tropical South American continent, especially in the dry season. Adding to that is the strongly pronounced dipole in precipitation in the dry groups, with drying over the Caribbean and northern South America and wetting over the equatorial Pacific that reaches further east in the dry group compared to the wet group. Indicating the

eastward migration of the Walker circulation; with rising air and precipitation over the Pacific equatorial region (upward branch of the Walker circulation) and subsiding air and dry conditions over tropical South America and the Caribbean (downward branch of the Walker circulation). This is backed up by looking at the wind vectors in Figure 17. These wind vectors show divergence where the downward branch is located and an increase in trade winds over the Pacific.

Contrarily the wet group shows weaker warming over the equatorial Pacific, a less pronounced dipole in precipitation and no clear divergence patterns. Suggesting a milder eastward migration of the Walker circulation.

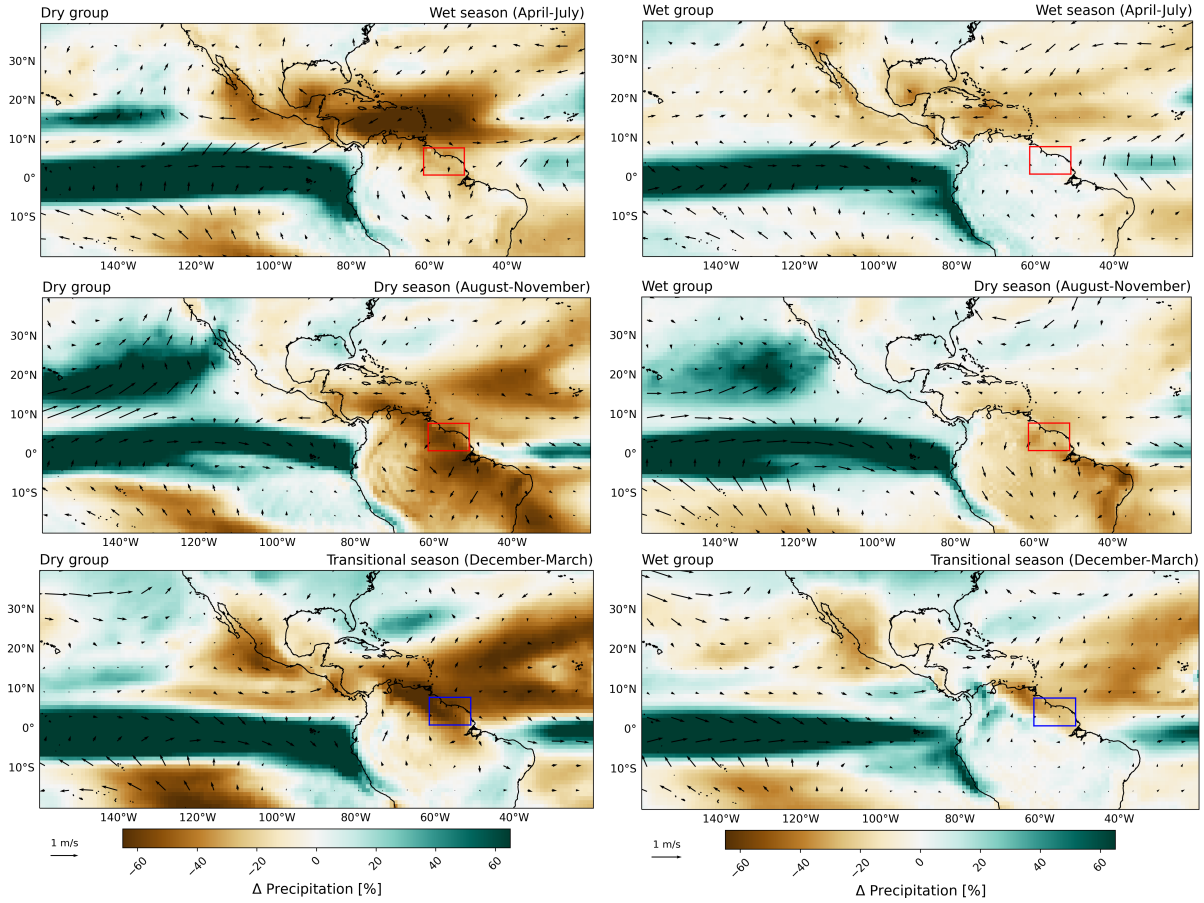

Figure 17: Projected relative precipitation change (colors, in %) and absolute wind change at 925 hP a (vectors, in m/s) for the dry (left panels) and wet (right panels) groups of models under SSP5-8.5 in 2100 (matched warming). The figures display changes for the AMJJ season in the upper panels, the ASON season in the middle panels and the DJFM season in the lower panels. The data presented depicts the multimodel mean of the 10 CMIP6 models in each group (The groups are calculated for SSP5-8.5 in 2100). The figures show the raw (i.e., not downscaled) multimodel mean of the 10 CMIP6 models in each group. The red box indicates the Guyanas region.

In Figure 16 a significant reduced warming of the Northern Atlantic is visible. This suggests the influence of the Atlantic Meridional Overturning Circulation (AMOC). The AMOC is a mechanism that consists of the transport of large volumes of water within the Atlantic ocean. The AMOC transports heat across the equator and is therefore partly responsible for the temperature difference in the Atlantic between the Northern

and Southern hemisphere. The Northern hemisphere is slightly warmer than the southern hemisphere, resulting in the ITCZ position just north of the equator (Buckley and Marshall, 2016).

CMIP6 simulations show a decline of the AMOC strength over the Atlantic. This decline in AMOC strenght would cause a southward migration of the ITCZ, which results in drier conditions over Suriname.

Summarizing the wet/dry groups of Suriname are characterized by a strong/weak El-Nino response together with a strong/weak reduction of the AMOC. How El-Nino and AMOC will change in the future is a topic of current world-wide research.

6 Sea level rise

Sea level scenarios are created by summing up all of the processes that contribute significantly to long-term sea-level change and that are not part of natural sea-level variations. Hence, the scenarios do not contain natural yearly variations induced by winds and the fluctuation of ocean currents. The incorporated processes responsible for sea-level rise are:

- Global thermosteric sea-level due to the net ocean heat uptake caused by global warming.
- Ocean dynamic sea-level (ODSL) associated with a change in ocean currents and a changed distribution of heat and salt across the oceans that is forced by global warming through changes in evaporation and precipitation, heat uptake, heat release, and windpatterns.
- The addition of glacial meltwater.
- Melting of the Antarctica icesheet.
- Melting of the Greenland icesheet.
- Changes in landwater storage.
- Glacial Isostatic Adjustment (GIA); the ongoing movement of land due to the lifting of the weight of past ice masses.

6.1 Data

Monthly sea level from satellite altimetry was downloaded from the Copernicus Marine Data Store. Globally averaged sea level from satellite altimetry was downloaded from AVISO. The sea level record from the tide gauges of Puerto Rico and French Guyana were downloaded from the Permanent Service for Mean Sea Level (PSMSL).

Information on the method of the sea level scenarios can be found in Chapter 4 of van Dorland et al. (2024).

6.2 Observations

The closest location with tide gauge data in the PSMSL database to Suriname is the Ile Royal tide gauge in front of the coast of French Guyana (Figure 18b). For comparison to a longer timeseries of tide gauge data, the tide gauge from Magueyes Islan, Puerto Rico is also added (Figure 18a). From both data series a rising sea level trend is clear. The tide gauge data was compared to satellite altimetry observations close to the locations of the tide gauges. The satellite altimetry data and tide gauge data follow the same pattern and therefore we can assume the satellite altimetry data to be usefull for the coast of Suriname as well.

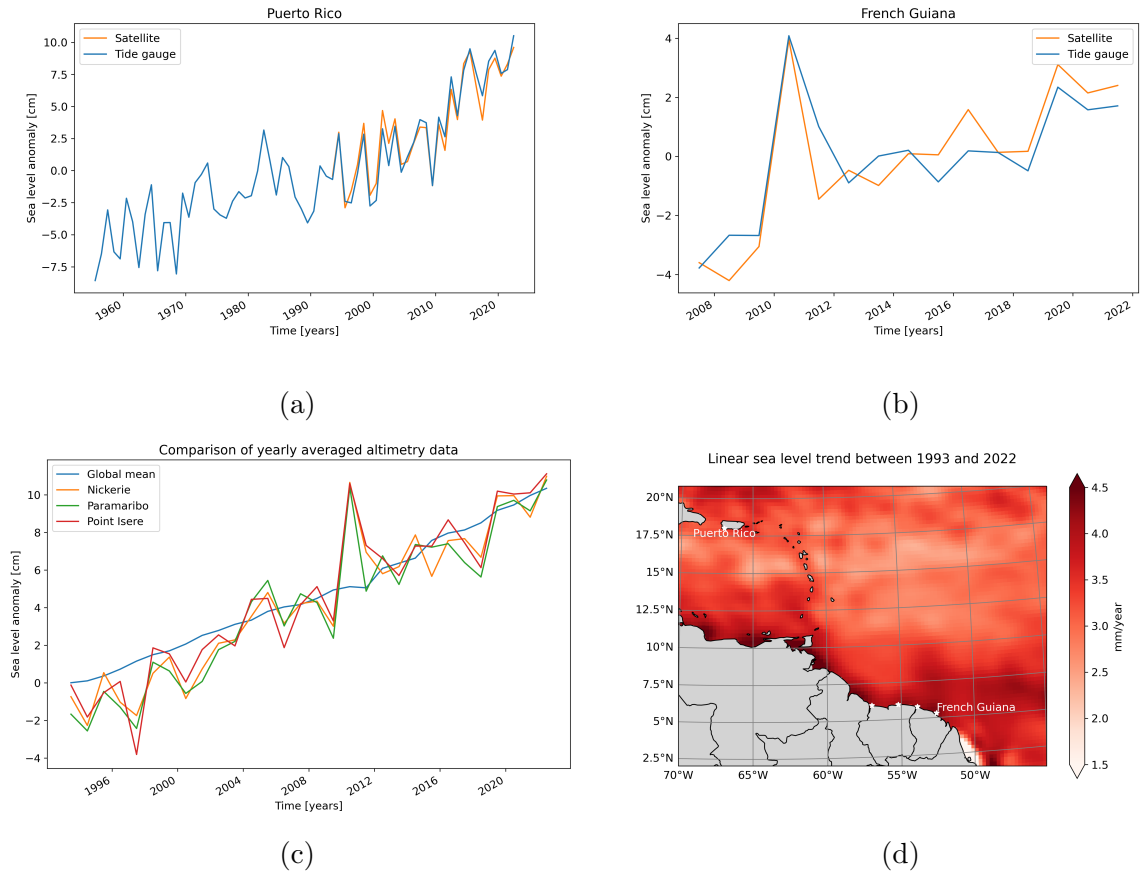

Figure 18: (a) Yearly averaged observed sea level at Puerto Rico from tide gauge (Magueyes Island) and satellite altimetry. (b) Yearly averaged observed sea level at French Guyana from tide gauge (Ile Royale) and satellite altimetry. (c) Yearly averaged sea level for three locations at the coast of Suriname and globally averaged from satellite altimetry. (d) Map of linear sea level trend in mm/yr.

The linear trend for the satellite altimetry data near the Puerto Rico tide gauge is 3.2 ±0.5 mm/yr for the period 1993-2021. The tide gauge linear trend at the same location is a little higher; 3.8 ±0.5 mm/yr for the period 1993-2021. The long-term linear tide gauge trend for the period 1955-2022 is 2.0 ±0.2 mm/yr, which indicates an acceleration of sea level rise in the region.

The satellite altimetry observations of three locations at the coast of Suriname are shown in Figure 18c. Here a similar increasing trend in sea level is visible, with a remarkable jump of around 7 cm from 2009 to 2010 after which sea level gets back to the long term rising trend. The linear trend over the period 1993-2022 is 4.1 ±0.3 mm/yr at Nickerie, 4.2 ±0.3 mm/yr at Paramaribo, and 4.2 ±0.3 mm/yr at Point Isere. These rates are faster than the average global sea level rate of 3.4 mm/yr.

6.3 Projections

The sea level scenarios for Suriname are shown in Figure 19. Future median sea level projections for 2100, compared to the reference period 1995-2014, are about +45 cm under SSP1-2.6 and about +78 cm in SSP5-8.5. There is a large uncertainty around these values. Especially since dynamics in historic sea level (Figure 18d) show faster trends

around the coasts that coarse climate projections are not capturing. Rates of relative sea level for 2100 under SSP1-2.6 and SSP5-8.5 are about 2.8 mm/yr and 14.5 mm/yr. The sea level does not stop rising after 2100 and in Figure 20 the possible scenarios towards 2300 are made visible, indicating the large impact a seemingly small rate of increase can have in the far future. All the projection numbers for 2050 and 2100 can be found in Table 2.

In Figures 19-20 there are also three so-called low-likelihood high impact scenarios (LLHI) shown. Some physical mechanisms that are not yet included in standard models could potentially accelerate the speed of sea level rise and are presented with the dotted lines in the figurse. More information on the low-likelihood high impact scenarios can be found in Chapter 4 of van Dorland et al. (2024).

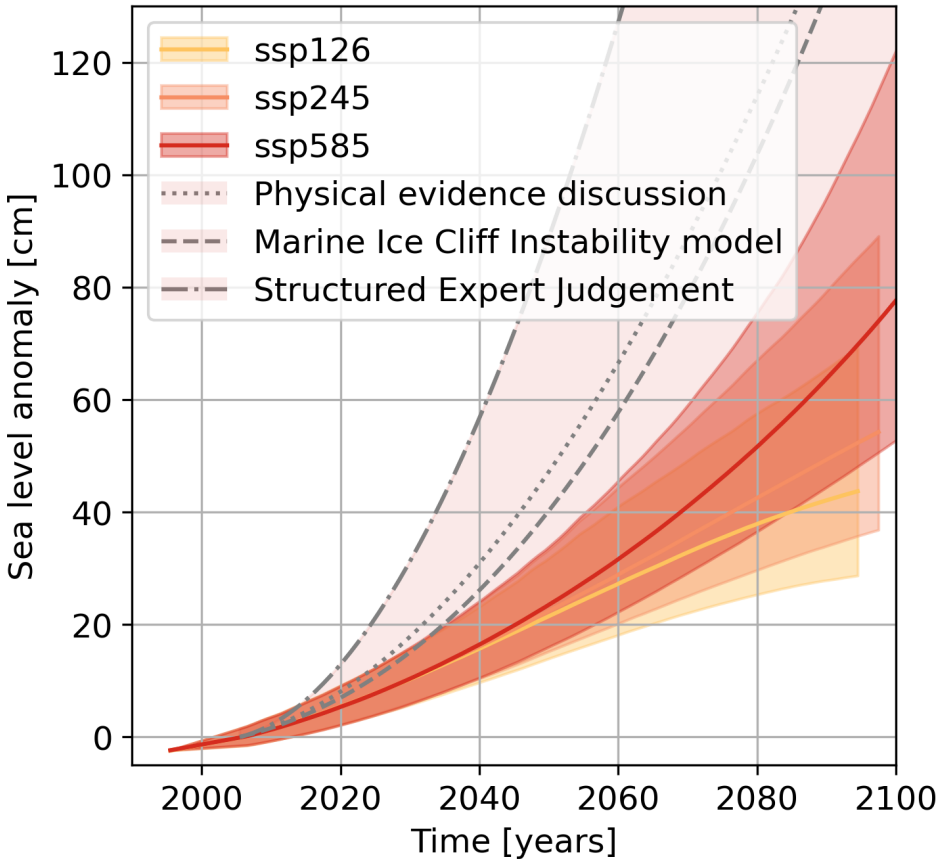

Figure 19: Sea-level scenarios at the coast of Suriname for the SSP1-2.6, SSP2-4.5 and SSP5-8.5 emission scenarios compared to the reference period 1995-2014. The median and 5th to 95th percentile range are shown. Grey lines represent the low probability high impact scenarios (see chapter 4 of van Dorland et al. (2024)).

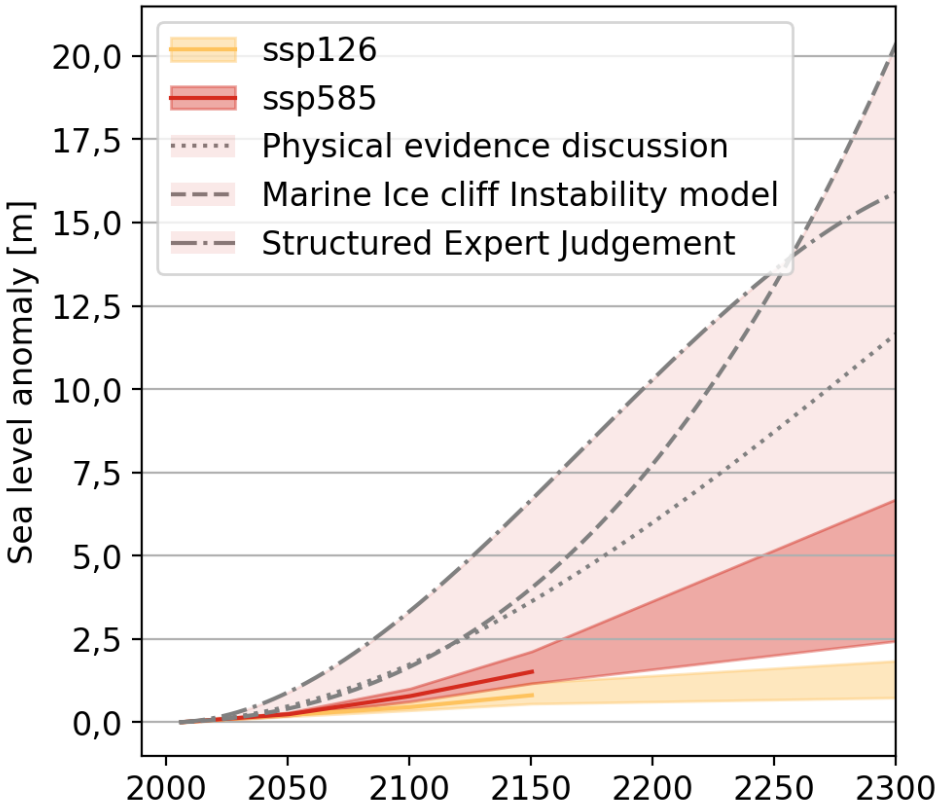

Figure 20: Sea-level scenarios at the coast of Suriname for the SSP1-2.6, SSP2-4.5 and SSP5-8.5 emission scenarios compared to the reference period 1995-2014. The median and 5th to 95th percentile range are shown. Grey lines represent the low probability high impact scenarios (see chapter 4 of van Dorland et al. (2024)).

2050			
	SSP1-2.6	SSP2-4.5	SSP5-8.5
Global steric	8 (5 to 10) cm	8 (6 to 11) cm	9 (6 to 12) cm
Ocean Dynamic Sea Level	4 (-1 to 9) cm	4 (-1 to 8) cm	3 (-3 to 8) cm
Glaciers	3 (2 to 5) cm	4 (2 to 5) cm	4 (3 to 6) cm
Landwater	1 (1 to 2) cm	1 (1 to 2) cm	1 (1 to 2) cm
Greenland	2 (2 to 4) cm	3 (2 to 4) cm	3 (2 to 5) cm
Antarctica	4 (0 to 13) cm	3 (-1 to 14) cm	4 (-1 to 13) cm
GIA	-1 (-1 to -1) cm	-1 (-1 to -1) cm	-1 (-1 to -1) cm
Total	22 (14 to 32) cm	23 (15 to 34) cm	24 (16 to 34) cm
Rate total	5.8 (4.3 to 9.2) mm/yr	6.4 (5.0 to 10.7) mm/yr	7.6 (5.9 to 10.9) mm/yr
Rate total (anomalies, rounded)	2.0 (0.0 to 5.0) mm/yr	2.0 (1.0 to 6.0) mm/yr	3.0 (2.0 to 7.0) mm/yr
2100			
Global steric	15 (10 to 20) cm	21 (14 to 27) cm	32 (22 to 42) cm
Ocean Dynamic Sea Level	4 (-1 to 10) cm	5 (-1 to 11) cm	4 (-4 to 12) cm
Glaciers	8 (4 to 11) cm	10 (6 to 14) cm	14 (9 to 20) cm
Landwater	2 (1 to 4) cm	2 (1 to 4) cm	2 (1 to 4) cm
Greenland	7 (4 to 10) cm	8 (5 to 14) cm	14 (8 to 26) cm
Antarctica	10 (-1 to 37) cm	11 (-1 to 46) cm	13 (-3 to 54) cm
GIA	-1 (-1 to -1) cm	-1 (-1 to -1) cm	-1 (-1 to -1) cm
Total	45 (29 to 74) cm	56 (38 to 93) cm	78 (53 to 123) cm
Rate total	2.8 (1.1 to 7.9) mm/yr	6.4 (3.4 to 13.2) mm/yr	14.5 (8.4 to 27.7) mm/yr
Rate total (anomalies, rounded)	-1.0 (-3.0 to 4.0) mm/yr	2.0 (-1.0 to 9.0) mm/yr	10.0 (4.0 to 24.0) mm/yr

Table 2: Median and 5th to 95th percentile range of individual sea level contributions in 2050 and 2100 relative to 1995-2014 for the Surinam coast. The row "Rate total" is the rate of sea level independent of the reference period while the row "Rate (anomalies, rounded)" is the anomaly compared to the rate during the reference period which is 4.2 mm/yr. LLHI scenarios are not included in this table.

7 Discussion

The method for providing the climate scenarios for Suriname for the variables of temperature, precipitation and wind offer various advantages, but also has its limitations. One of the strong features of the scenarios is that they are based on a multi model approach (instead of a single model realization), and therefore capture a broad range of uncertainties in the climate response. This is important given the rather large role of model uncertainty in future precipitation (see the work of Hawkins and Sutton (2011) as introduced in the Introduction). However there are also known limitations and systemic biases to the CMIP6 models that impact the climate scenarios.

One of these biases of the CMIP6 models is a tendency of the models for El Niño conditions compared to the observations over the past decades that show a La Niña tendency (Bayr et al., 2014; Seager et al., 2019). It is still unclear within the scientific community whether this difference in trends is driven by internal variability or that biases in the CMIP6 models are the cause of this difference (Seager et al., 2019; Wills et al., 2022). If there is indeed a bias in the models this would suggest that the amount of drying in the Suriname scenarios is potentially overestimated.

Another known bias in climate models is the double ITCZ bias (Tian and Dong, 2020; Si et al., 2021). Climate models have been shown to project the ITCZ, a narrow band of tropical heavy precipitation, at the wrong location compared to historical observations or even a double ITCZ band. This double ITCZ pattern can be seen in Figure 21, where there is a positive precipitation bias (more precipitation in CMIP6 compared to GPCP) visible in the South Eastern Pacific and a negative bias in the eastern equatorial Pacific.

With the location of Suriname just north of the equator, where the ITCZ traverses twice a year over the country, the location of the ITCZ is of high importance for the development of climate scenarios for Suriname. In general the ITCZ is positioned too far towards the south. The wet and dry group models show similar ITCZ bias patterns.

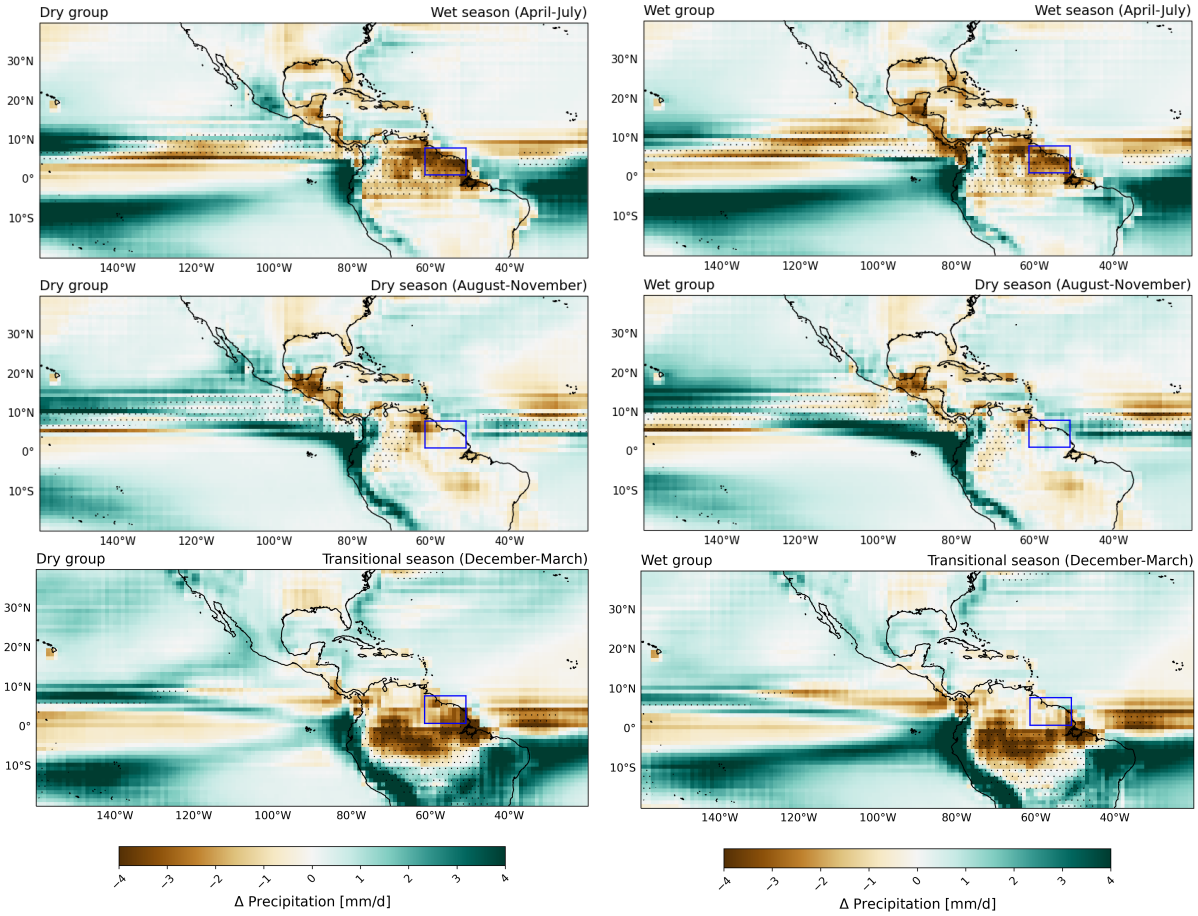

Figure 21: Difference between CMIP6 models and GPCP dataset Huffman et al. (2009)

Precipitation extremes are not incorporated in this climate scenarios report. As can be seen in Figure 9 the end of the tail distributions for precipitation are overfitted during the QDM statistical downscaling. In general CMIP6 GCM's are not capable of simulating precipitation extremes. Processes like intense convective rainshowers of short-duration are not resolved within the resolution of GCM's. Chapter 5 of van Dorland et al. (2024) goes deeper into the explanation why direct use of precipitation extremes from GCM model runs is not advisable. Combined with the known biases of climate models mentioned above we do not feel confident enough to make assumptions about the values of precipitation extremes for Suriname. For an indication; the raw CMIP6 data shows for Suriname an increase in extreme precipitation values (Rx1day, Rx5day) for the wet group and not a clear signal in extreme precipitation for the dry group, while showing less wet days for both groups (R10mm,R20mm).

In general a tendency towards more extreme precipitation events with rising temperatures is expected. The capacity of air to hold water vapour goes up with rising temperature (O'Gorman, 2015). The rate of the atmospheric moisture increase with temperature is approximately 7% per °C. This is also known as the Clausius-Clapeyron (CC) moisture

rate. Intense short-duration rainshowers may even show patters up to a 14 % per °C increase (Lenderink et al., 2017). Even when reductions in mean precipitation are expected, the precipitation extremes are likely to increase.

Another limitation in the development of the climate scenarios for Suriname was the availability of long, accurate and complete data sets for the region. The southern part of Suriname lacks datasets with high enough quality to accurately perform the statistical downscaling. This has limited the scenarios end product for that region. Another improvement would have been to have a high-resolution gridded dataset specific for the area that can be used to produce gridded end results.

8 Conclusion and recommendations

In general Suriname should prepare for warmer and drier conditions and a significant amount of sea level rise. Although we do not explicitly compute extreme values within this report, both temperature and precipitation extremes are expected to increase in the future. This means that for Suriname both droughts and flooding could become more frequent problems in the future.

To calculate extreme precipitation values, regional climate modelling efforts are necessary. With convective permitting models at higher resolution more research about changes in extreme precipitation can be made (van Dorland et al., 2024). Also longer time series of (sub-)daily climatic parameters could improve the ability to create future scenarios for extremes.

One of the important take-aways of this report should be the discrepancy between the wet-trending and dry-trending models during the wet season (AMJJ). If the ensemble mean of all CMIP6 models is taken, the mean change would be close to zero. However with the scenario pathways analyzed in this report it is shown that in order to make Suriname and its society resilient to future climate change both an increase and a decrease in precipitation during the wet season (AMJJ) should be anticipated.

To fully understand the dynamics of future climate change for Suriname and the region, trends in the changes of large circulation processes like ENSO and the ITCZ should be investigated further.

Also, further study upon the impact of cascading climate effects is necessary; e.g. rising temperatures in combination with days without wind or decreasing precipitation amounts, or rising sea levels in combination with increasing precipitation amounts and an increase in windspeed.

References

Bayr, T., Dommenget, D., Martin, T., and Power, S. B. (2014). The eastward shift of the Walker Circulation in response to global warming and its relationship to ENSO variability. *Climate Dynamics*, 43(9):2747–2763.

Bovolo, C. (2010). Using reanalysis data to establish the precipitation and temperature regime of data poor areas: the Guianas of South America. In *Role of hydrology in managing consequences of a changing global environment*. British Hydrological Society.

Brotons, M., Haarsma, R., Bloemendaal, N., de Vries, H., and Allen, T. (2024). Drivers of Caribbean precipitation change due to global warming: analyses and emergent constraint of CMIP6 simulations. *Climate Dynamics*, 62(5):3395–3415.

Buckley, M. W. and Marshall, J. (2016). Observations, inferences, and mechanisms of the Atlantic Meridional Overturning Circulation: A review. *Reviews of Geophysics*, 54(1):5–63. _eprint: https://onlinelibrary.wiley.com/doi/pdf/10.1002/2015RG000493.

Cai, W., McPhaden, M. J., Grimm, A. M., Rodrigues, R. R., Taschetto, A. S., Garreaud, R. D., Dewitte, B., Poveda, G., Ham, Y.-G., Santoso, A., Ng, B., Anderson, W., Wang, G., Geng, T., Jo, H.-S., Marengo, J. A., Alves, L. M., Osman, M., Li, S., Wu, L., Karamperidou, C., Takahashi, K., and Vera, C. (2020). Climate impacts of the El Niño–Southern Oscillation on South America. *Nature Reviews Earth & Environment*, 1(4):215–231.

Cannon, A. J., Sobie, S. R., and Murdock, T. Q. (2015). Bias Correction of GCM Precipitation by Quantile Mapping: How Well Do Methods Preserve Changes in Quantiles and Extremes? *Journal of Climate*, 28(17):6938–6959. Publisher: American Meteorological Society Section: Journal of Climate.

Córdova, M., Célleri, R., and van Delden, A. (2022). Dynamics of Precipitation Anomalies in Tropical South America. *Atmosphere*, 13(6):972. Number: 6 Publisher: Multidisciplinary Digital Publishing Institute.

de Valk, C. (2020). Standard method for determining a climatological trend. Technical Report TR-389, KNMI, De Bilt.

Dieng, D., Cannon, A. J., Laux, P., Hald, C., Adeyeri, O., Rahimi, J., Srivastava, A. K., Mbaye, M. L., and Kunstmann, H. (2022). Multivariate Bias-Correction of High-Resolution Regional Climate Change Simulations for West Africa: Performance and Climate Change Implications. *Journal of Geophysical Research: Atmospheres*, 127(5):e2021JD034836. _eprint: https://onlinelibrary.wiley.com/doi/pdf/10.1029/2021JD034836.

Feigenwinter, I., Kotlarski, S., Casanueva, A., Fischer, A., Schwierz, C., and Liniger, M. A. (2018). Exploring quantile mapping as a tool to produce user-tailored climate scenarios for Switzerland. Technical Report No. 270, MeteoSwiss.

Fredriksen, H.-B., Berner, J., Subramanian, A. C., and Capotondi, A. (2020). How Does El Niño–Southern Oscillation Change Under Global Warming—A First Look at CMIP6. *Geophysical Research Letters*, 47(22):e2020GL090640. Publisher: John Wiley & Sons, Ltd.

Hausfather, Z. and Peters, G. P. (2020). Emissions – the 'business as usual' story is misleading. *Nature*, 577(7792):618–620.

Hawkins, E. and Sutton, R. (2011). The potential to narrow uncertainty in projections of regional precipitation change. *Climate Dynamics*, 37(1-2):407–418.

Hersbach, H., Bell, B., Berrisford, P., Biavati, G., Horányi, A., Muñoz Sabater, J., Nicolas, J., Peubey, C., Radu, R., Rozum, I., Schepers, D., Simmons, A., Soci, C., Dee, D., and Thépaut, J.-N. (2023). ERA5 monthly averaged data on pressure levels from 1940 to present.

Huffman, G. J., Adler, R. F., Bolvin, D. T., and Gu, G. (2009). Improving the global precipitation record: GPCP Version 2.1. *Geophysical Research Letters*, 36(17):2009GL040000.

IPCC (2021). The physical science basis. Technical report.

Koole, E. C. (2023). Potential sources of predictive skill of seasonal precipitation forecasts for Suriname: A study on the dynamics of seasonal precipitation in Suriname with the help of moisture tracking and Sea Surface Temperature correlations. [Master's Thesis, Technical University Delft].

Lenderink, G., Barbero, R., Loriaux, J. M., and Fowler, H. J. (2017). Super-Clausius–Clapeyron Scaling of Extreme Hourly Convective Precipitation and Its Relation to Large-Scale Atmospheric Conditions. Section: Journal of Climate.

McPhaden, M. J., Santoso, A., and Cai, W. (2020). *El Niño Southern Oscillation in a Changing Climate*. John Wiley & Sons.

O'Gorman, P. A. (2015). Precipitation Extremes Under Climate Change. *Current Climate Change Reports*, 1(2):49–59.

Schneider, U., Hänsel, S., Finger, P., Rustemeier, E., and Ziese, M. (2022). GPCC Full Data Monthly Version 2022 at 0.25°: Monthly Land-Surface Precipitation from Rain-Gauges built on GTS-based and Historic Data: Globally Gridded Monthly Totals. Artwork Size: min. 20 MB - max. 300 MB per gzip archive (10 years per archive) Pages: min. 20 MB - max. 300 MB per gzip archive (10 years per archive).

Seager, R., Cane, M., Henderson, N., Lee, D.-E., Abernathey, R., and Zhang, H. (2019). Strengthening tropical Pacific zonal sea surface temperature gradient consistent with rising greenhouse gases. *Nature Climate Change*, 9(7):517–522. Publisher: Nature Publishing Group.

Seager, R., Henderson, N., Cane, M., Zhang, H., and Nakamura, J. (2021). Atmosphere–Ocean Dynamics of Persistent Cold States of the Tropical Pacific Ocean. *Journal of Climate*, 34(13):5195–5214. Publisher: American Meteorological Society Section: Journal of Climate.

Si, W., Liu, H., Zhang, X., and Zhang, M. (2021). Double Intertropical Convergence Zones in Coupled Ocean-Atmosphere Models: Progress in CMIP6. *Geophysical Research Letters*, 48(23):e2021GL094779. _eprint: https://onlinelibrary.wiley.com/doi/pdf/10.1029/2021GL094779.

Solaun, K., Alleng, G., Flores, A., Resomardono, C., Hess, K., and Antich, H. (2021). State of the Climate Report: Suriname. *IDB Publications*. Publisher: Inter-American Development Bank.

Tian, B. and Dong, X. (2020). The Double-ITCZ Bias in CMIP3, CMIP5, and CMIP6 Models Based on Annual Mean Precipitation. *Geophysical Research Letters*, 47(8):e2020GL087232. _eprint: https://onlinelibrary.wiley.com/doi/pdf/10.1029/2020GL087232.

van der Wiel, K., Beersma, J., van den Brink, H., Krikken, F., Selten, F., Severijns, C., Sterl, A., van Meijgaard, E., Reerink, T., and van Dorland, R. (2024). KNMI'23 Climate Scenarios for the Netherlands: Storyline Scenarios of Regional Climate Change. *Earth's Future*, 12(2):e2023EF003983. _eprint: https://onlinelibrary.wiley.com/doi/pdf/10.1029/2023EF003983.

van Dorland, R., Beersma, J., Bessembinder, J., Bloemendaal, N., Drijfhout, S., Groenland, R., Haarsma, R., Homan, C., Keizer, I., Krikken, F., van Meijgaard, E., Meirink, J. F., Overbeek, B., Reerink, T., Selten, F., Severijns, C., Siegmund, P., Sterl, A., de Valk, C., van Velthoven, P., de Vries, H., van Weele, M., and Schreur, B. W. (2024). KNMI National Climate Scenarios 2023 for the Netherlands. Scientific report WR-23-02, De Bilt.

Wills, R. C. J., Dong, Y., Proistosecu, C., Armour, K. C., and Battisti, D. S. (2022). Systematic Climate Model Biases in the Large-Scale Patterns of Recent Sea-Surface Temperature and Sea-Level Pressure Change. *Geophysical Research Letters*, 49(17):e2022GL100011. _eprint: https://onlinelibrary.wiley.com/doi/pdf/10.1029/2022GL100011.

9 Supplementary material

CMIP6 models	wet model group	dry model group
ACCESS-ESM1-5	X	
AWI-CM-1-1-MR	X	
MPI-ESM1-2-LR	X	
MPI-ESM1-2-HR	X	
NorESM2-MM	X	
MIROC-ES2L	X	
HadGEM3-GC31-LL	X	
NorESM2-LM	X	
IPSL-CM6A-LR	X	
BCC-CSM2-MR	X	
CESM2		
FGOALS-g3		
CESM2-WACCM		
MIROC6		
CanESM5		
UKESM1-0-LL		
CNRM-ESM2-1		
GFDL-ESM4		
MRI-ESM2-0		
CMCC-CM2-SR5		X
CNRM-CM6-1		X
ACCESS-CM2		X
EC-Earth3-Veg		X
KACE-1-0-G		X
EC-Earth3		X
CNRM-CM6-1-HR		X
NESM3		X
INM-CM5-0		X
INM-CM4-8		X

Table 3: CMIP6 models included in the scenarios

Royal Netherlands Meteorological Institute

PO Box 201 | NL-3730 AE De Bilt
Netherlands | www.knmi.nl